EZW Coding with Improved Execution Time on the Basis of Descendant Scanning of Zero-tree Roots

A Thesis submitted in partial fulfilment of the Requirements for the award of degree of

Master of Engineering
in
Electronics Instrumentation and Control

Submitted by

ANANT RAJ SINGH
(Roll No. 801051002)

Under the Guidance of

Mr. Moon Inder Singh
Assistant Professor

Ms. Ruchika Lamba
Lecturer

Department of Electrical and Instrumentation Engineering
Thapar University
(Established under the section 3 of UGC act, 1956)
Patiala, 147004, Punjab, India

July 2012

DECLARATION

I hereby certify that the work which is being presented in the thesis entitled "**EZW Coding with Improved Execution Time on the Basis of Descendant Scanning of Zero-tree Roots**" in partial fulfilment of the award of degree of **Master of Engineering** in **Electronics Instrumentation and Control** Submitted in the Electrical and Instrumentation Engineering Department, Thapar University , Patiala is an authentic record of my own work carried under the supervision of Mr. Moon Inder Singh Assistant Professor, Department of Electrical and Instrumentation Engineering , Thapar University , Patiala, Punjab and Ms. Ruchika Lamba, Lecturer, Department of Electrical and Instrumentation Engineering, Thapar University , Patiala, Punjab.

Date: 16/7/12

Anant Raj Singh
801051002

I certify that the above statement made by the student is correct to the best of my knowledge and belief.

Mr. Moon Inder Singh
Assistant. Professor
Department of Electrical and
Instrumentation Engineering
Thapar University, Patiala
Punjab

Ms. Ruchika Lamba
Lecturer
Department of Electrical and
Instrumentation Engineering
Thapar University, Patiala
Punjab

Countersigned By

Dr. Smarajit Ghosh
Head Of Department
Department of Electrical and
Instrumentation Engineering
Thapar University, Patiala, Punjab

Dr. S.K. Mohapatra
Dean of Academic Affairs
Thapar University, Patiala
Punjab

31/7/12

Abstract

Compression is a very important aspect of maintaining database systems. Thus efficiency of compression systems is important. In todays world the transfer of data too is done in a compressed manner. The bit stream is optimized. One such way is embedded transmission scheme in which the compressed low bit rate information is transmitted first and then the higher rates follow. In this scheme even if some part of bit stream is not received, information corresponding to lower bit rate can be decoded. Thus in such transmission schemes both transmitting and encoding time are important. Embedded Zero-tree Wavelet (EZW) encoding is one such technique for embedded transmission and compression of images. EZW for images has been used to form a video coder also.

The main objective of this thesis is to implement and improve EZW coding. The thesis proposes a coding scheme based on EZW, with improved execution time and compression ratio using some constraints. The improvement in the present coding is done by assuming that most of the coefficients values lying in the decomposition subband are low and near to zero. Thus they need not to be checked again and again for significance. This saves encoding time in the proposed coding scheme, based on EZW. The proposed coding scheme reduces the execution time by 2 sec. and compression ratio almost by 2% in 7 iterative passes without any degeneracy in the decoded image as compared with standard EZW coding. Improvement of 1 sec. more can be made in execution of 8 successive passes, if a fall of around 1 dB is allowed in the decoded image of proposed coding as compared to the decoded image of EZW coding at the 8^{th} pass.

The first part of this thesis is dedicated in knowing discrete wavelet transform which is the base of the present coding and then the EZW coding itself is covered in detail. In next part the theory to improve the present coding is stated and then the improved coding scheme is proposed. Later, results are brought out on various images in support of the theory and constraints are defined. Finally, future aspects of research with respect to proposed coding scheme are introspected.

Acknowledgements

The first and foremost thanks in completion of my thesis go to my supervisor Mr. Moon Inder Singh; for having faith in me and motivating and guiding me in every positive way whenever I got stuck.

Special thanks, with gratitude go to my co-supervisor Ms. Ruchika for the support and help given to me during the tenure of this thesis work; and guiding me where ever necessary.

I would like to thank Dr. Smarajit Ghosh, Professor and Head of the Department of Electrical & Instrumentation Engineering, Thapar University Patiala for providing all facilities in completion of this thesis.

I would like to thank all my friends, especially Mr. Rohit Gupta for helping and understanding me throughout my stay at the University.

One person who deserves to be thanked is Mr. Anil Vashisht; who constantly pushed me forward towards the spiritual goal and tolerated me with love.

Lastly, I would like to thank my Parentage and family for cultivating a sense of research in me, in both material and spiritual world.

TABLE OF CONTENTS

LIST OF FIGURES

LIST OF TABLES

Chapter 1

Introduction

1.1 Overview

Database compression is a very important aspect in all the fields. Frequently a database comprises of images that are two dimensional signals. The compression is important for the purpose of storage and for data transfer. So after compression lesser amount of coded data has to be sent, though maintaining a good representation of the original uncoded data. Such is required in case of Biometrics, which involves images of face, fingerprints etc. for the purpose of detection and recognition; also for Biomedical Imaging which involves MRI, CAT-Scan, X-Ray Scans etc. for diagnosis of disease; and also in general Imaging Applications such as web browsing, multimedia, photography etc.

Progressive image transmission over the channel involves embedded coding in which the lower bit rate image is embedded first in the output bit stream and then the higher bit rates follow thereafter. In such codings, each successive pass of transmission the information is added to already existing information. Thus with the passage of transmission a higher bitrate image is obtained. Even if the bit stream is truncated at any point according to the requirement of decoder, still an image can be generated corresponding to lower bit-rate. Embedded Zero-tree Wavelet (EZW) is one such technique for embedded coding and compression of all sorts of images.

1.2 Motivation

As progress took place in research in the field of image processing its applications developed. Such as in biometrics in which in today's world the data of all the citizens of the nation is stored. Also in forensic where biometric records of criminals are maintained requires suitable compression. Medical field itself gives a vast area for the purpose of compression where scanning and diagnosis of disease can be done in different centers across the world. Such application requires transfer of the data that is desired to be in the most optimum compression possible.

Wavelet transform is an emerging area in field of research in applied mathematics. They have undergone a drastic transformation during the last twenty years in the applied application field. Wavelets are a step closer to reality than its counterpart transforms hence they have always been in the eyes of the researchers. Wavelets provide a very dynamic field of application and are applicable to image too.

1.3 Objective of Thesis

The objective of the work carried out is as follows

- To study and implement the Wavelet based encoding of Images based on the multi-resolution theory.
- To implement the progressive transmission technique, Embedded Zero-Tree Wavelet Compression algorithm of Images as explained by J.M. Shapiro in his transaction.
- To improve the overall aspects of algorithm as much possible; including the time and space complexity.

1.4 Organization of Thesis

Chapter 1 gives a brief introduction and overview of the work. It highlights the objective that is desired to be achieved.

Chapter 2 of the thesis gives an introduction to discrete wavelet transforms sufficiently enough for the purpose of engineering applications. It also presents a literature review necessary for the purpose of the research carried out.

Chapter 3 of the thesis discusses Embedded Zero-tree Wavelet Coding in detail.

Chapter 4 of the thesis discusses the proposed work in which the EZW is improved on the basis of descendant coefficients scanning and encoding.

Chapter 5 discusses the results obtained by applying the improved algorithm.

Chapter 6 gives the conclusion of the thesis. It also explores the future aspect of the subject.

Chapter 2

Discrete Wavelet Transform

2.1 Introduction to Wavelets

Wavelets were first introduced and applied in the field of seismology – which is branch of science that deals with signals emanating from the core of the earth towards the crust of the earth, such as earthquakes.

Wavelets are mathematical functions that cut up data into different frequency components, and then study each component with a resolution matched to its scale. They have advantages over traditional Fourier methods in analyzing physical situations where the signal contains discontinuities and sharp spikes. Wavelets were developed independently in the fields of mathematics, quantum physics, electrical engineering, and seismic geology. Interchanges between these fields during the last ten years have led to many new wavelet applications such as image compression, turbulence, human vision, radar, and earthquake prediction. Often signals we wish to process are in the time-domain, but in order to process them more easily other information, such as frequency, is required. Mathematical transforms translate the information of signals into different representations. For example, the Fourier transform converts a signal between the time and frequency domains, such that the frequencies of a signal can be seen. However the Fourier transform cannot provide information on which frequencies occur at specific times in the signal as time and frequency are viewed independently. To solve this problem, the Short Term Fourier Transform (STFT) introduced the idea of windows through

which different parts of a signal are viewed. For a given window in time, the frequencies can be viewed. However, Heisenberg's Uncertainty Principle states that as the resolution of the signal improves in the time domain, by zooming on different sections, the frequency resolution gets worse. Ideally, a method of multi-resolution is needed, which allows certain parts of the signal to be resolved well in time, and other parts to be resolved well in frequency. The power and magic of wavelet analysis is exactly this multi-resolution.

2.2 A brief history of Wavelets

Jean Mortlet, an engineer, was initially giving a better way to geologist to search for oil. But this started a new revolution termed wavelets. He described *wavelets of constant shape* which were later known as *Mortlet wavelets.* He brought out the theory of dilating, compressing or shifting the Mother Wavelet in time.

Mortlet yet unsatisfied with the theory worked with *Alex Grossmann*, a physicist form Marseilles and produced the proof that waves could be reconstructed from their wavelet decomposition. They published a paper in 1984 and first used the term 'wavelets'. *Yves Meyer* when heard about there work realized a relationship between Mortlet's wavelets and other existing previous mathematical work. He infact, counted 16 such papers before the work of Mortlet was published.

Meyer introduced the concept and feature of *orthogonality* in wavelets which is foundation concept of wavelets today.

In 1986, *Stephane Mallat*, a former student of Meyer linked the theory of wavelets to the existing literature on *subband coding* and *quadrature mirror* filters which are the image processing community's versions of wavelets. Mallat's work very importantly introduced the concept of *multiresolution* which is a keystone to wavelet theory.

The final revolution was in the area of wavelets was brought by *Ingrid Daubechies* in 1987, when she at New York University and later at AT&T Bell laboratories, discovered a whole new class of wavelets which were not only orthogonal but which could be implemented using short and simple digital filters. Combining the work of Daubechies and Mallat there is a simple orthogonal transform which could be calculated on modern digital computers [1].

2.3 Basic definitions

Some of the basic definitions are defined to understand the theory of wavelets.

2.3.1 Orthogonal functions

Two real functions $f_1(t)$ and $f_2(t)$ are said to be orthogonal if and only if

$$\int_{-\infty}^{\infty} f_1(t)\, f_2(t)\, dt = 0 \tag{2.1}$$

The example of two orthogonal functions can be sine and cosine functions in the same interval. Unit vectors of Cartesian plane $\vec{\imath}, \vec{j}, \vec{k}$ also contribute to orthogonal vectors.

2.3.2 Dyadic Sampling

Dyadic Sampling is termed as sampling of alternate values of the signal. In Dyadic downsampling the alternate terms in the signal are dropped. In Dyadic upsampling zero-padding is done alternately between the samples of the signal. The word dyadic is derived from the word *dia* i.e. meaning two. Dyadic upsampling is shown in figure 2.1.

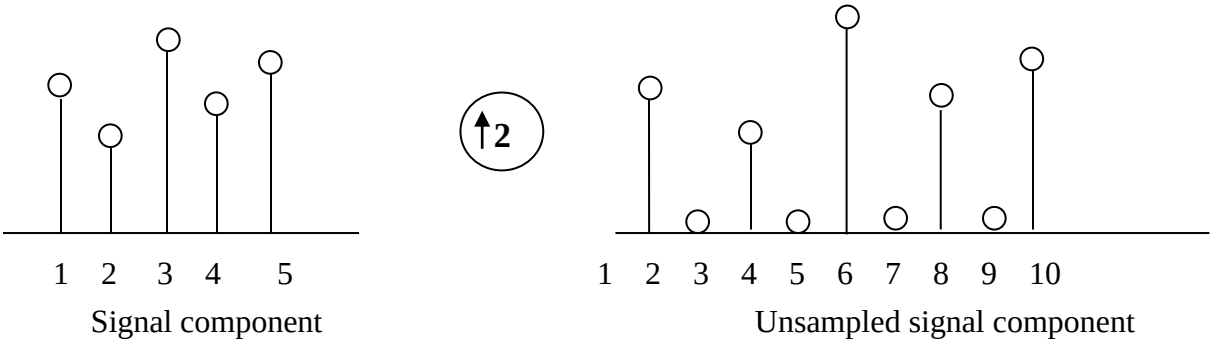

Figure 2.1 Components after upsampling

2.3.3 Basis Functions and CWT

Any vector in 3-dimensional space can be represented as $\vec{V} = a\vec{\imath} + b\vec{j} + c\vec{k}$. $\vec{\imath}, \vec{j}, \vec{k}$ are called as bases of space $\mathbb{R}^3$. By this it is meant that any vector in space $\mathbb{R}^3$ can be represented using vectors $\vec{\imath}, \vec{j}, \vec{k}$. The unit vectors $\vec{\imath}, \vec{j}, \vec{k}$ also span the space $\mathbb{R}^3$. By changing the scalars *a ,b, c*

continuously a new set of vectors are generated each time in the space of $\mathbb{R}^3$. This is expressed as,

$$\underbrace{Span}_{a,b,c}\left(\overrightarrow{a\vec{\imath}+b\vec{j}+c\vec{k}}\right) \equiv \mathbb{R}^3 \tag{2.2}$$

A basis function for a transform which measures the full range of frequency content of a signal at a time instant, would need to have compact support (a limited interval of non-zero values) in the time domain and frequency domain. This basis function should be time translatable (shift to measure the signal at different times, i.e. Shifting) and frequency scalable (expands and contract to measure different signal frequencies, i.e. Scaling). The wavelet functions,

$$\Psi_{a,b}(t) = a^{-1/2}\,\Psi\left(\frac{t-a}{b}\right) \quad a \in R^+, b \in R \tag{2.3}$$

were developed as these basis functions for the Continuous Wavelet Transforms (CWT); where b is the location parameter (shifting) and a is the scaling parameter. Thus the translation and scaling of the wavelet, defines the corresponding function in the corresponding wavelet space whose transform has to be obtained.

Thus a CWT is defined as,

$$CWT_f(a,b) = \int_{-\infty}^{\infty} \Psi_{a,b}\,(t)\,f(t)\,dt \tag{2.4}$$

i.e.,

$$CWT_f(a,b) = \int_{-\infty}^{\infty} f(t)\,a^{-1/2}\,\Psi\left(\frac{t-a}{b}\right) \tag{2.5}$$

According to Eq. (2.5), for every (a , b) we have a wavelet transform coefficient, representing how much the scaled wavelet is similar to the function at location $t = (b/a)$.

2.4 Discrete Wavelet Transform

In order to develop the DWT, the wavelet functions must first be discretized. Thus the wavelet functions in Eq. 2.3 are modified with the following relations:

$$a = a_0^{-j};\ b = kb_0a_0^{-j}; \quad j,k \in Z;\ a_0 > 1;\ b_0 \neq 0 \tag{2.6}$$

Where, Z is the set of integers. The value of a_0 and b_0 are arbitrarily set to 2 and 1, respectively. Thus, $a = 2^{-j}$ and $b = k2^{-j}$ are used to discretize the Continuous Wavelet Transform. As *j* gets smaller, the scaling factor, *a,* increases which expands the wavelet function. The translation step size *b/k,* also increases as *m* becomes smaller. Thus the step size is scaled same as the scaling factor. With this discretization, low frequency and high frequency signals can be comparably analyzed. The wavelet functions in Eq. 2.3 become,

$$2^{j/2}\,\Psi\left(2^{j}t-k\right);\quad m,n\in Z \tag{2.7}$$

These wavelet functions form an orthonormal basis *of* $L^2(R)$, which is defined as the function space of square integrable functions in the theory of wavelets. This means that the function over which the wavelet transform is to be applied should belong to the $L^2(R)$ space of which the corresponding wavelet is the basis function.

Hence the resulting transform becomes,

$$d_{m,n} = \int_{-\infty}^{\infty} f(t)\,2^{j/2}\,\Psi\left(2^{j}t-k\right)dt\ ,\quad f(t)\in L^2\,(R) \tag{2.8}$$

2.5 Multiresolution Approach

S. Mallat gave the theory of multiresolution approach in wavelets [2] and his work was published as a transaction in IEEE. The concept of *nested space* in wavelet theory is the basic of this multiresolution approach which is a specific feature of wavelet transforms.

2.5.1 Nested space

If the concept of nested space is to be stated without going into deep details, it is – the coarse scale is itself derived from the finer scale previous to it i.e. the coarser scale space is a subset of the finer scale space. In other words, the successive coarser spaces are nested in finest scale space.

Let V_j denote the space of j^{th} scale. Then the original space V_3 can be decomposed into a lower resolution sub-space V_2, the difference between V_3 and V_2 can be represented by the complementary sub-space W_2. Similarly, we can continue to decompose V_2 into V_1 and W_1. Figure 2.2 shows 3-level decomposition in this manner. Thus for N-level decomposition,

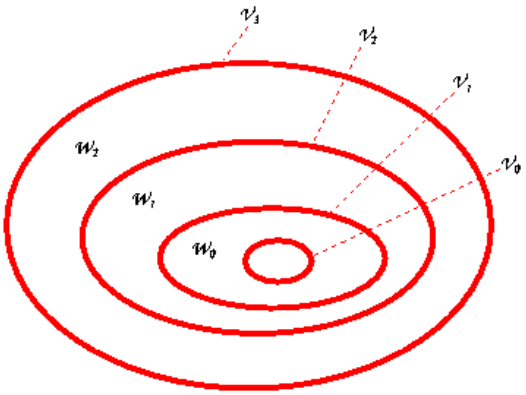

Figure2.2 Nested function spaces spanned by the wavelet and scaling functions.

N+1 sub-space with one coarsest resolution sub-space V_0 and N difference sub-space W_i are obtained; where i is from 1 to N. Each digital signal in the space V_3 can be decomposed into some components in each sub -spaces. This could be stated in a generalized way, as in Eq. (2.9)

$$\dots V_{-1} \subset V_0 \subset V_1 \subset V_2 \dots \subset V_\infty \subset L^2(R) \tag{2.9}$$

In many cases, it's much easier to analyze these components rather than analyze the original signal itself.

2.5.2 Filter Banks and relation with $\phi(t)$ and $\Psi(t)$

As also stated before, the work of I. Daubechies [3] made wavelet transforms simple which could be implemented using discrete filters. These were short duration filters and could be generated easily.

It should be noticed that wavelet function $\Psi(t)$ and the corresponding scaling function $\phi(t)$ are themselves generated from these discrete filters. Much detail is outside the scope of this thesis.

The relation between the filters *h(n)* and *g(n)* with wavelet and scaling function derived from Eq. (2.8) is given by the *refinement relations*,

$$\phi(t) = \sum_{k=0}^{N-1} h(k)\sqrt{2}\,\phi(2t-k) \tag{2.10}$$

$$\Psi(t) = \sum_{k=0}^{N-1} g(k)\sqrt{2}\,\phi(2t-k) \tag{2.11}$$

In direct approach of designing wavelets of specific *tap* or *support* first the coefficients of these filters are obtained after applying some specific constraints on them; such as those of

othogonality, normalization and that of Moments. The way of obtaining Daubechies tap 6 (db6) wavelet is shown below for the purpose of demonstration.

Constraints for Daubechies' 6 Tap Scaling Function [4]

For N = 6,

Constraint Type	*Constraints on Coefficients*
Normalization	$c_0 + c_1 + c_2 + c_3 + c_4 + c_5 = 2$
Square Normalization	$c_0^2 + c_1^2 + c_2^2 + c_3^2 + c_4^2 + c_5^2 = 2$
Double Shift Orthogonality	$c_0c_2 + c_1c_3 + c_2c_4 + c_3c_5 = 0$ $c_0c_4 + c_1c_5 = 0$
Vanishing Moments	p=0, p=1, p=2

After solving, we obtain {h(k)} as follows:

h(0) = 0.3326705529500825

h(1) = 0.8068915093110924

h(2) = 0.4598775021184914

h(3) = - 0.1350110200102546

h(4) = - 0.0854412738820267

h(5) = 0.0352262918857095

g(k) can be obtained by reversing the coefficients of h(k) and changing the sign of alternate position.

Thus with the help of refinement relation wavelet and scaling function can be obtained and are shown in figure 2.3.

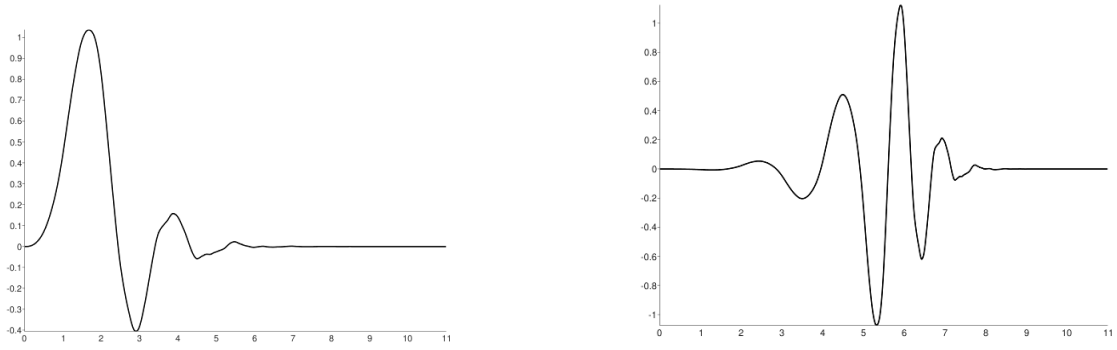

Figure2.3 Scaling and wavelet function of db'6

It can been shown that the wavelet and the scaling functions corresponding to the j^{th} scale i.e. w.r.t. the basis of space V_j can be calculated by generalizing the refinement relations given in Eq. (2.10) and (2.11) for different scales. The relations are given as,

$$\phi(2^j t - k) = \sum_{m=2k}^{2k+N-1} h(m-2k)\sqrt{2}\,\phi(2^{j+1}t - m) \tag{2.12}$$

$$\Psi(2^j t - k) = \sum_{m=2k}^{2k+N-1} g(m-2k)\sqrt{2}\,\phi(2^{j+1}t - m) \tag{2.13}$$

If s_j and d_j are taken as the scaling and wavelet coefficients at the scale *j*, then the relations (2.12) and (2.13) can be written as,

$$s_j = \sum_{m=2k}^{2k+N-1} h(m-2k)\, s_{j+1}(m) \tag{2.14}$$

$$d_j = \sum_{m=2k}^{2k+N-1} g(m-2k)\, s_{j+1}(m) \tag{2.15}$$

By solving the relations (2.14) and (2.15) mathematically, it can be shown that the *relations are equivalent to convolution followed by downsampling of even terms in the output series*. It means that the relations can be implemented simply, rather than involving complex mathematical manipulations.

Thus Eq. (2.14) can be visualized as illustrated in figure 2.4

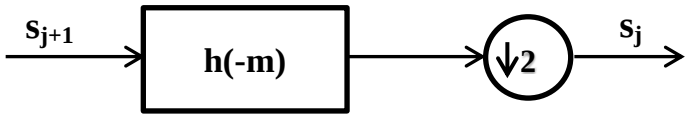

Figure 2.4 Relation between s_{j+1} and s_j

In the same way Eq. (2.15) can be seen as illustrated in figure 2.5

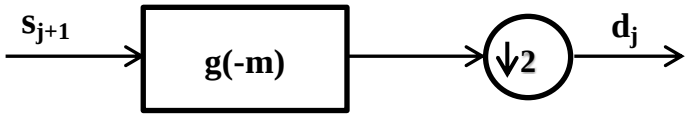

Figure 2.5 Relation between s_{j+1} and d_j

Finally, the analysis i.e. the decomposition of of signal in V_{j+1} into sum of two signals; one in space V_j (corresponding to s_j) and the other in W_j (corresponding to d_j) is visualized and exhibited in Figure 2.6.

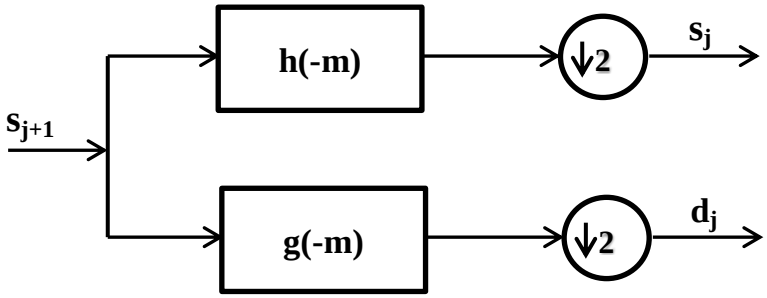

Figure 2.6 Relation between s_{j+1}, s_j and d_j

The procedure illustrated above is actually the Decomposition of Signals using Wavelet Transform. This is one-stage decomposition only. In 'filter bank theory', it is called as two band analysis. The sequence of coefficients $\{s_j(k)\}$ can be further decomposed into sequences $\{s_{j-1}(k)\}$ and $\{d_{j-1}(k)\}$ using the relations (2.14) and (2.15). At each stage, the length of the sequences approximately halves due to decimation by 2 i.e. dyadic downsampling, after convolution. Figure 2.7 shows two-stage, two-band analysis.

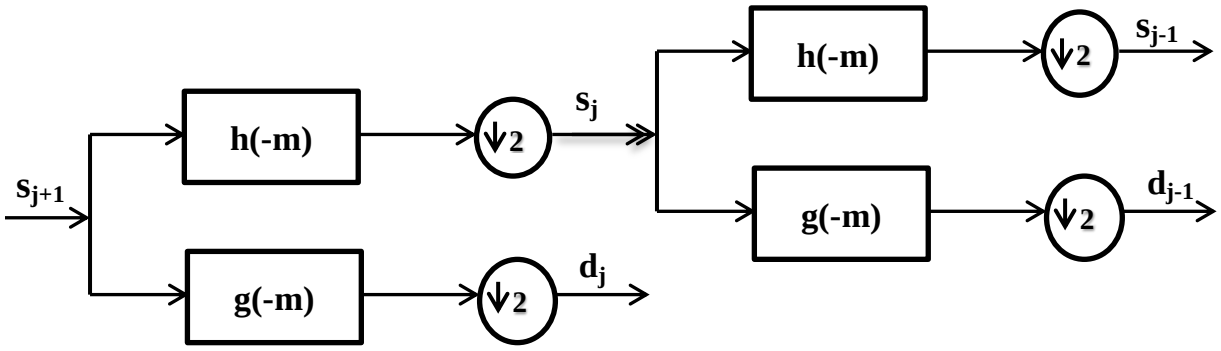

Figure 2.7 Two-band analysis of signals uptill second stage

The filters represented by h(-m) and g(-m) are low pass and high pass FIR filters respectively. The sum of number of coefficients in sequence $\{s_j(k)\}$ and $\{d_j(k)\}$ are almost equal to the number of coefficients in the signal sequence $\{s_{j+1}(k)\}$. Hence, it is possible that no information is lost in the splitting of frequency bands and the original sequence can be recovered from this decomposed sequence.

2.5.3 Signal Reconstruction

Where wavelet analysis involves filtering and downsampling, the wavelet reconstruction process or synthesis consists of upsampling and filtering. Upsampling is the process of lengthening a signal component by inserting zeros between samples. The signal reconstruction is opposite of signal decomposition.

Mathematically the signal reconstruction can be stated as,

$$s_{j+1}(k) = \sum_m s_j(m)\, h(k-2m) + \sum_m d_j(m)\, g(k-2m) \qquad (2.16)$$

Since the translation quantity is *2m*, each of *h(k)* and *g(k)* is not getting multiplied with *s* and *d* terms. For a given *k*, either odd indexed terms of *h(k)* and *g(k)* or even indexed terms of *h(k)* and *g(k)* are participating in the summation. So, to make it a perfect convolution sum, without affecting the final result, simply upsample (add 'zero' between each term in *s* and *d*) and do the ordinary convolution. This can be visualized as shown in figure 2.8 and figure 2.9.

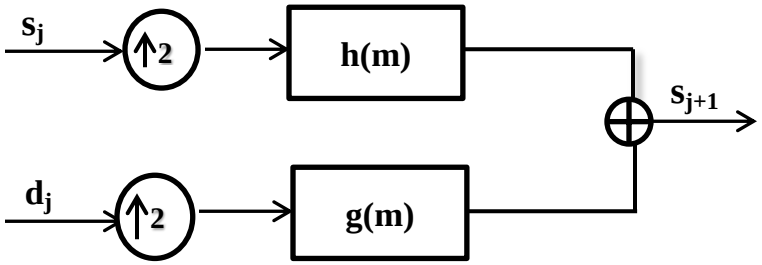

Figure 2.8 Synthesis of s_{j+1} from s_j and d_j

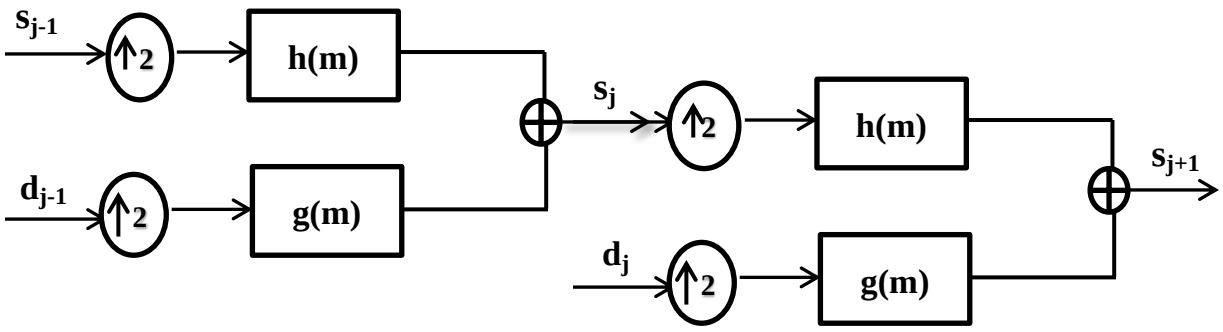

Figure 2.9 Two-stage synthesis process.

2.5.4 Perfect Matching Filters

Wavelet analysis filters *{h(-m), g(-m)}* decompose the signal into various frequency bands and wavelet synthesis filters *{h(m), g(-m)}* reconstruct the decomposed signal back into the original signal. Set of such system of filters are called perfectly matching filters. Since *h(m)* and *g(m)* are orthogonal in vectorial sense, and analysis filters are mirror image of synthesis filters, these filters are also called as **quadrature mirror filters** or **QMF**.

2.6 Wavelet Coding of Images

Images are 2-D signals. The wavelet coding of image is done in similar fashion, as in 1-D signals. In case of images, the discrete wavelet transform is applied both along the rows and columns to obtain the approximations and details. The process is illustrated in figure 2.10.

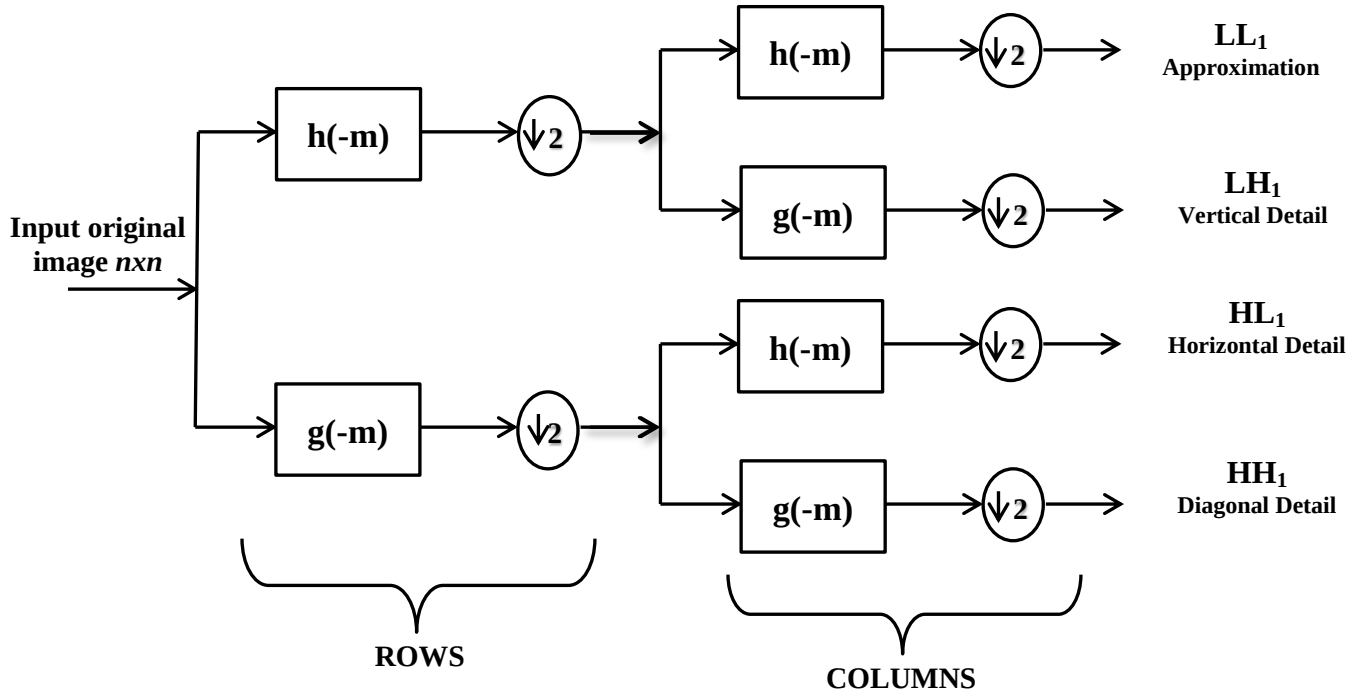

Figure 2.10 One-stage 2-D wavelet decomposition of image.

2.6.1 Image Decomposition

The discrete wavelet transform is obtained by passing the signal to low and high pass decomposition filters which gives approximation and detail coefficient values at each level of decomposition. Same thing is done in the case of image. But the image carries information varying along two dimensions. Thus approximation and detail coefficients have to be extracted

from both the directions. For this purpose first the low-pass and high-pass filters are first moved over the rows of the image and the result is decimated by a factor of two, as shown in figure 2.10. This divides the wavelet decomposition subband specifically into two parts. One subband contains the low frequency information i.e. approximation of the rows and the other contains the high frequency information i.e. detail along the rows. This is depicted by figure 2.11 (a).

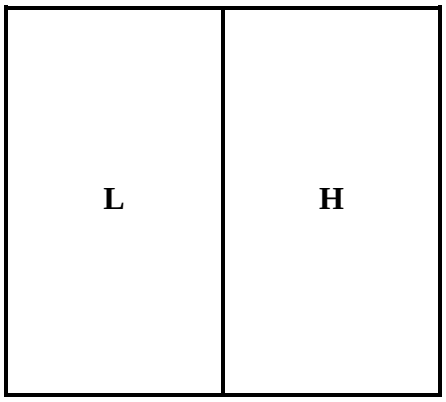

Figure 2.11 (a) – Subband after filtering and downsampling over rows

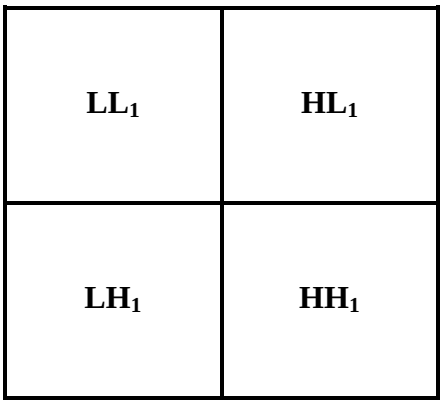

Figure 2.11 (b) – Subband after filtering and downsampling over both rows and columns

Now, the operation over columns of the image is applied. Upon the obtained subband, the decomposition process is again applied. They are again passed through high pass and low pass filter after which dyadic sampling is done. Thus, Subband is again decimated by a factor of two. This process of two-dimensional wavelet decomposition is clearly shown in figure 2.10. The subband obtained by passing low-pass filter over both rows and columns is divided into four, as shown in figure 2.11(b). LL_1, is approximation of the corresponding level. The remaining three subband are of detail – horizontal (HL_1), vertical (LH_1) or diagonal (HH_1); which is determined by direction in which the high pass filter is passed. This is explained as below.

LL_n – *Approximation:*	Low pass filter over rows and low pass filter over columns
HL_n – *Horizontal Detail:*	High pass filter over rows and low pass filter over columns
LH_n – *Vertical Detail:*	Low pass filter over rows and high pass filter over columns
HH_n – *Diagonal Detail:*	High pass filter over rows and high pass filter over columns

The resulting subband after one level of decomposition is divided into four parts which is due to dyadic sampling done on both rows and columns of the image after filtering process. Thus, if the original image is n x n the resulting each wavelet coefficient subband is of $n/2$ x $n/2$.

For obtaining the next level of decomposition, the Approximation is passed through the same 2-D filter bank in the same manner as stated above. This is shown in figure 2.12. Since the next level is obtained from the approximation of previous level, thus the previous approximation subband space is now divided into four spaces for the next level subbands. Schematically saying, in a layman language that the next level subbands are placed over the previous level approximation subband as they are generated from it and so on. This is shown in figure 2.13. Figure 2.14 shows one level, two levels and three level decomposition of "Cameraman" image.

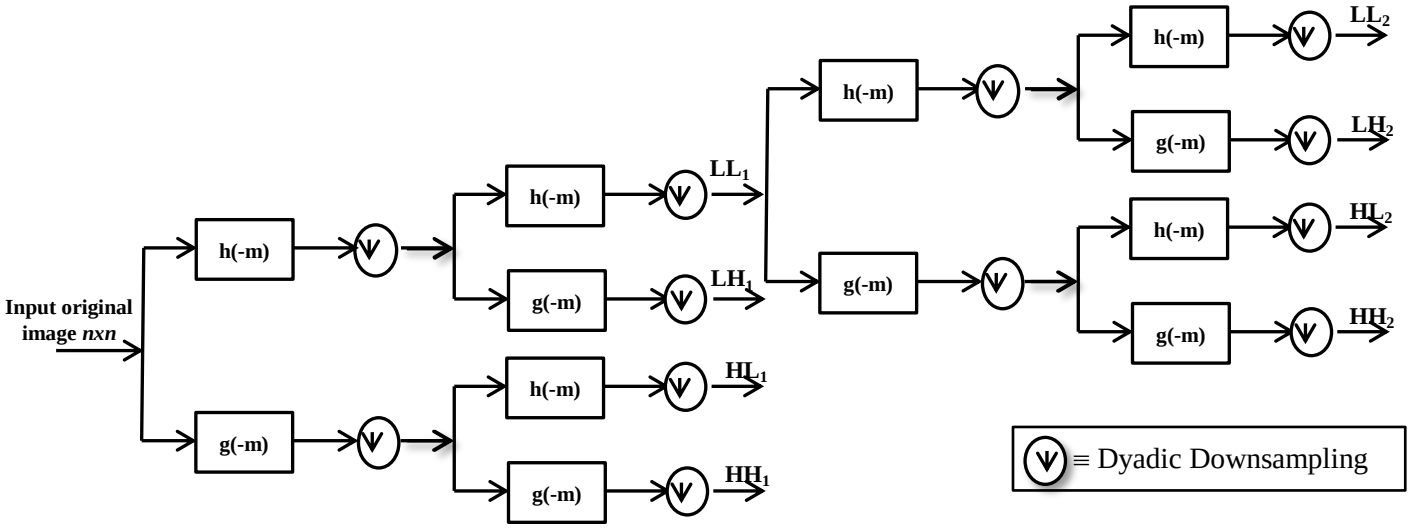

Figure 2.12 Two-stage 2-D wavelet decomposition of image.

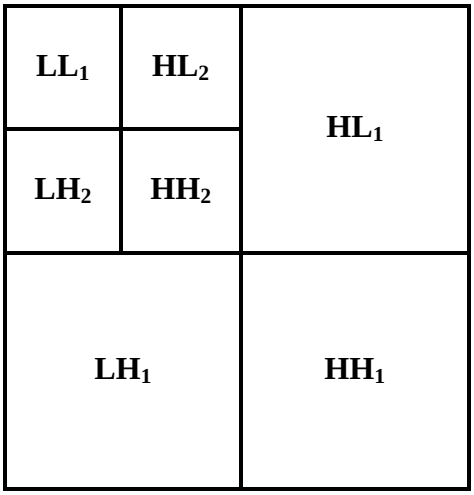

Figure 2.13 Second level Wavelet Decomposition Subband

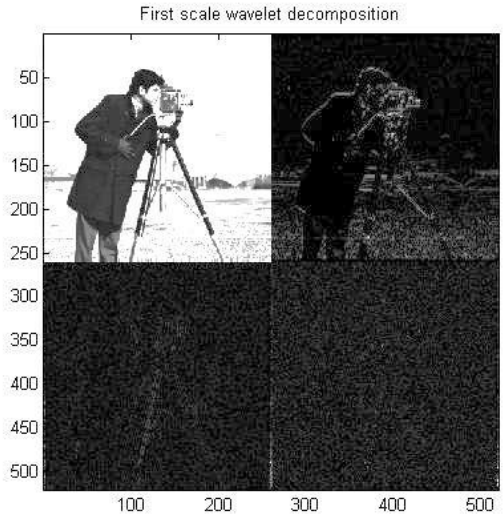

Figure 2.14(a) First level Wavelet Decomposition Subband of 'Cameraman' image

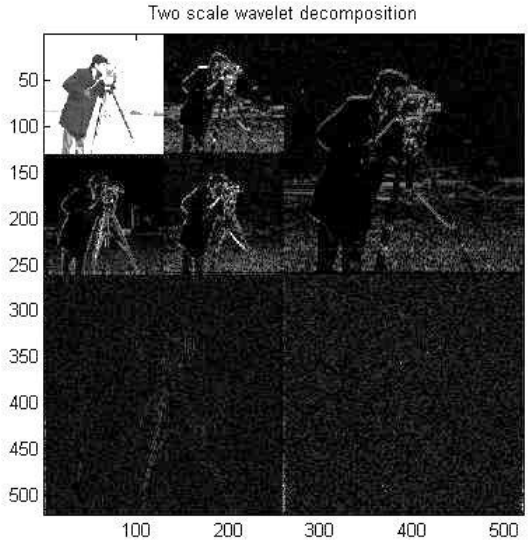

Figure 2.14(b) Second level Wavelet Decomposition Subband of 'Cameraman' image

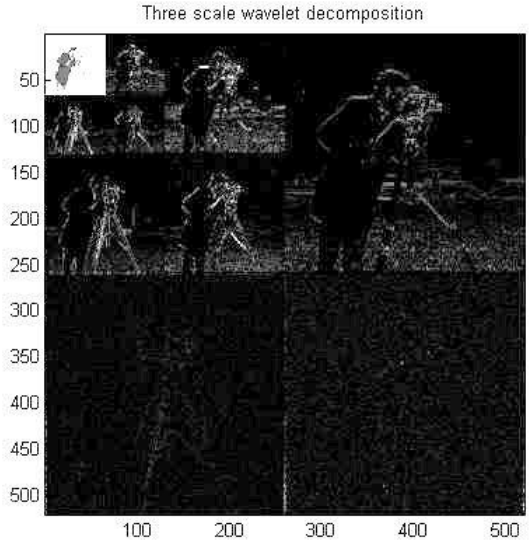

Figure 2.14(c) Third level Wavelet Decomposition Subband of 'Cameraman' image

2.6.2 Image Reconstruction

The image is reconstructed from the decomposed wavelet coefficient band by passing it through the synthesis filter banks followed by dyadic upsampling, as was done in case of 1-D signal reconstruction. The only difference here is that the filter bank is 2-Dimensional. The image reconstruction or Inverse Discrete Wavelet Transform of an image is just opposite of decomposition process. This is illustrated with the help of figure 2.15.

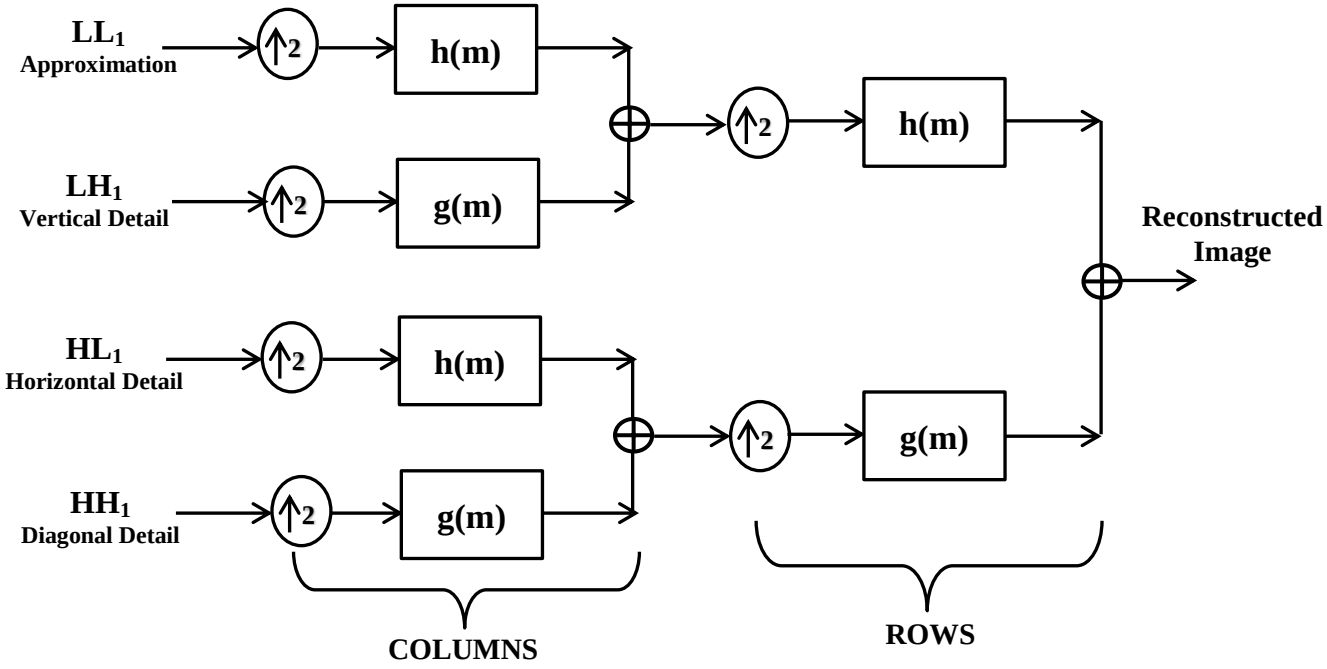

Figure 2.15 Two-stage 2-D wavelet reconstruction of image.

2.7 Literature Review

Wavelet transforms have always appeared mystical to researchers and scientists. **Ingrid Daubechies** has done a credible work in developing modern wavelets. Her *Ten Lectures on Wavelets* were published in 1992 in SIAM. **Stephane G. Mallat (1989)** applied the multiresolution on images through wavelets. He presented a work decomposing the image by wavelet transform in to sub-bands of approximation and details. A multiresolution representation provides a simple hierarchical framework for interpreting the image information. At different resolutions, the details of an image generally characterize different physical structures of the scene. Mallat provided a good amount of mathematical work to show that the difference of information between the approximation of a signal at the resolutions 2^{j+1} and 2^{j} can be extracted by decomposing this signal on a wavelet orthonormal basis. His work resulted in approximation of orthonormal basis of $L^2(R)$ and Mallats pyramidal multiresolution architecture. **Marc Antonini et.al (1992)** proposed a new coding scheme for images. This coding was based on transform coding of wavelet transforms. They introduced 2-Dimensional wavelet filter for encoding the image into wavelet domain. They also studied the statistical properties of wavelet coefficients across the subbands through their probability desnsity functions. They proposed a noise shaping bit allocation procedure by assuming that the high frequency details are less visible to eyes [5]. **J.M. Shapiro (1993)** introduced EZW which is the lossless compression technique based on wavelet subband coding. EZW depends upon parent-child relationships between various pixels in different subbands. The image pixels are highly correlated and in EZW children are coded in terms of their parents. The encoding and decoding could be stopped at any point yet high fidelity in compression is obtained [6]. **Armando Manduca (1995)** applied image compression using wavelet transforms on biomedical images [7]. **Amir Averbuch et.al (1996)** vector quantized the resulted coefficients of wavelet transform decomposition using LGB algorithm. They applied lossless compression such as Huffman or arithmetic coding to quantize the decomposition coefficients or their representative indices [8]. **Adrian Munteanu et.al (1999)** provided a technique for lossless compression of medical image coding. They extended the results using various developed wavelet algorithms in the engineering field and applied them on the medical images. They also compared the results [9]. **L. Kaur et.al (2003)** showed that most of the image energy is concentrated in one of the detail subband, either in vertical detail subband or horizontal detail subband in case of an Ultrasound Image. Thus improving PSNR at

higher compression ratios. They also compared the results using correlation coefficient on the images [10]. **Tang Guowei et.al (2007)** utilized the second generation wavelet transforms based on Lifting Scheme to perform embedded zero-tree wavelet coding. They improved the working of algorithm in scanning during quantization process by separating the high and low frequency bands and then manipulating them separately [11]. **Liu Xuhong et.al (2007)** proposed the improved coding by detecting wavelet trees which lie near edges in the subband. Their method of detection for such trees was based on variance of the tree. They proposed coding such trees with another separate symbol. Though the coding was improved but the coding cost also rose [12]. **Puja Bharti et.al (2009)** produced the comparative analysis of various wavelet based techniques used to compress medical images, for the purpose of transmission from remote area. They produced results on Ultrasound, CT and MRI Images [13].

Chapter 3

Embedded Zero-tree Wavelet Coding (EZW)

3.1 Introduction

Embedded Zero-tree Encoding was given by Jerome M. Shapiro, in his IEEE transaction. Since then the coding has been used widely. The coding has also formed the base of many other existing technologies, both in image and video compression. One such existing and widely used technology is MPEG-4 which is video codec based on EZW.

3.2 Embedded Coding

In Embedded coding, the information of lower importance is transmitted first. Later the information of higher importance is transmitted which adds to the earlier transmitted information. Thus an effective transmission scheme is generated.

Thus an embedded code contains lower rate codes "embedded" at the beginning of the bit stream; effectively, the bits are ordered according to their importance. Using an embedded code, an encoder can terminate the encoding at any point thereby allowing a target rate or distortion metric to be met exactly. Typically, some target parameter, such as bit count, is monitored in the encoding process. When the target is met, the encoding simply stops. Similarly, given a bit stream, the decoder can cease decoding at any point and can produce reconstructions corresponding to all lower-rate encodings.

In the case of images, all the encodings of the same image at lower bit rates are embedded in the beginning of the bit stream and the higher bit rates follow up till the target bit rate is achieved or the bit-budget is exhausted. Embedded coding is similar in spirit to binary finite precision representations of real numbers. All real numbers can be represented by a string of binary digits. For each digit added to the right, more precision is added.

3.3 Parent-child Relationship in Wavelet Image Sub-bands

In the previous chapter, the wavelet subbands were described in detail. The wavelet transform of the image generates subbands at each level; namely Approximation, Horizontal Detail, Diagonal Detail and Vertical Detail. Figure 3.1 shows the three level wavelet subband decomposition of the Cameraman image, obtained by using MATLAB. The higher level is always related to lower level as shown in earlier chapter through Eq. (2.9) – the coarse scale space is a subset of finer scale space.

But the inter-pixel relationship in the spatial image domain was not explored in deeply. The parent-child relationship or ancestor-descendant relationship, based on hierarchical orientation of levels is explored in this chapter. As it is known that the higher subband is placed over the approximation subband of the previous level, it is assumed that the highest level decomposition is at the highest hierarchical level.

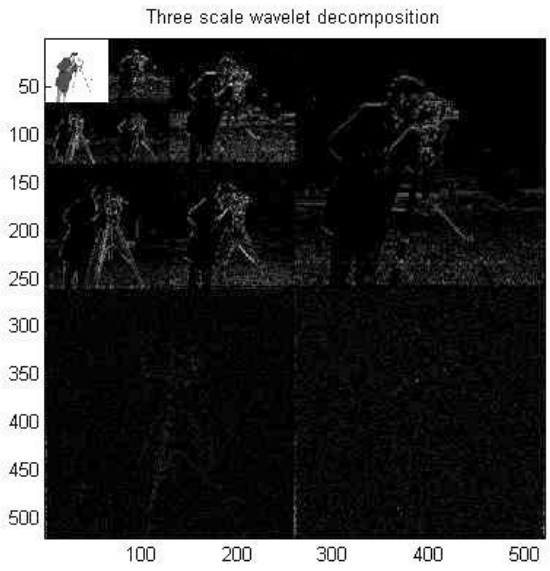

Figure3.1 Three-level decomposition of Cameraman Image.

The simple relation is that *a pixel in a coarser scale represents four pixels in the finer scale*, in 2x2 manner, except for the highest level approximation. The parent-child dependency in wavelet image subband coding is explained in the following steps.

- If the wavelet decomposition is done up till *N* levels, then the approximation existing in decomposition structure will belong to the highest level *N* only; as the rest of

approximations of lower levels have been decomposed to obtain the subband structure of the next higher level.

- Only in case of the N^{th} *level Approximation* i.e. LL_N *– there is a descendent each within the same level detail subbands occuring at the same spatial location.* This means that each pixel node of LL_N has a child or a pixel corresponding to it in HL_N, LH_N and HH_N; at the same spatial location. Thus for the lowest frequency approximation subband, the parent child relationship is defined such that each parent node has three children. This is clearly depicted in figure 3.2, which explains the dependencies in a three level decomposition structure.

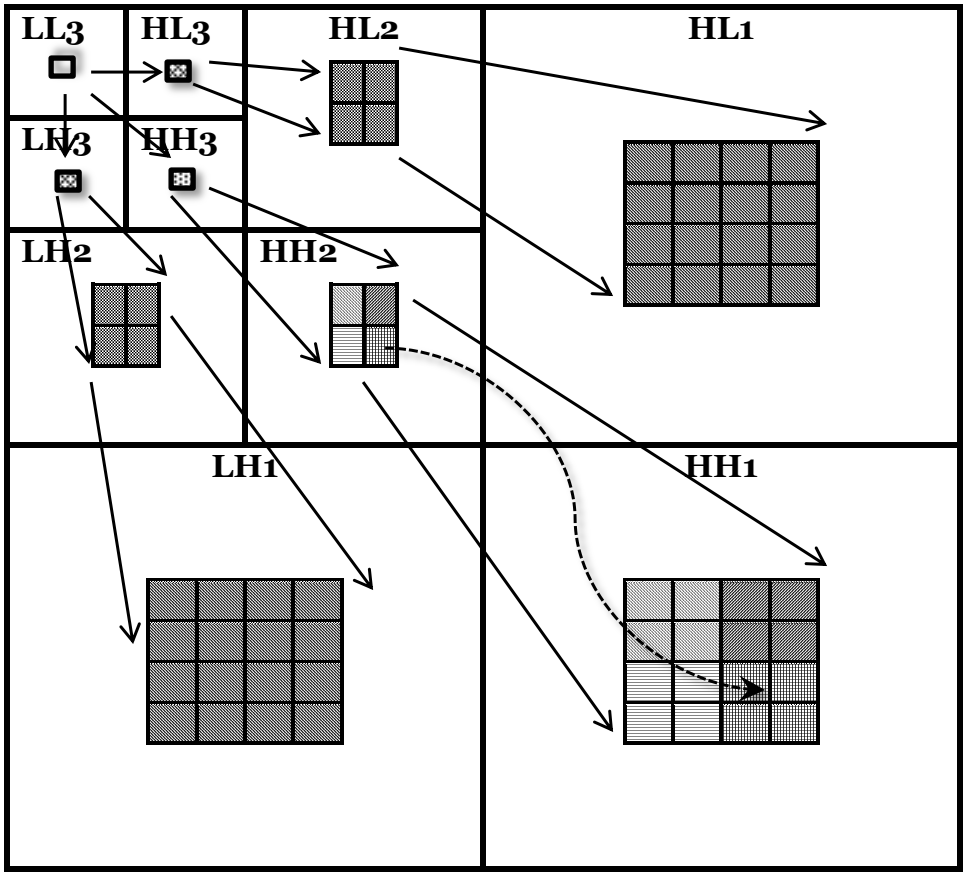

Figure3.2 Parent-Child dependencies of wavelet coefficients within the decomposition subband

- Details in decomposition subband do not have descendants within the same level subband. Their descendants always lie down in the finer scale i.e. lower the hierarchical level. Thus *each pixel node of detail subbands has four descendants down the*

hierarchical level, arranged in the 2x2 manner at the same spatial orientation. This has been clearly depicted in figure 3.2.

- This dependency is followed down the each hierarchical level within the wavelet image subband. Thus 2x2 pixel nodes are the descendants of a parent-pixel node of the higher level and the parents of 4x4 pixels i.e. 16 pixels in the lower level. This has been clearly shown in figure 3.2 with the help of straight arrows. But still in that 2x2 block each pixel is a parent of 2x2 block (within the 4x4 pixel block) down the level. This has been clearly depicted in figure 3.2 with the help of different shades and the dotted crocked arrow.
- The highest frequency subband i.e. HL_1, LH_1 and HH_1 do not have any descendants.
- The hierarchical tree grows in the similar fashion for any arbitrary N level decomposition.

Thus the parent-child dependencies in the image wavelet subband decomposition form a tree structure in which the higher decomposition level coefficient nodes are at the root level and the lower decomposition level coefficients are at the branch and leaf level. The tree formation is depicted in figure 3.3 shown below.

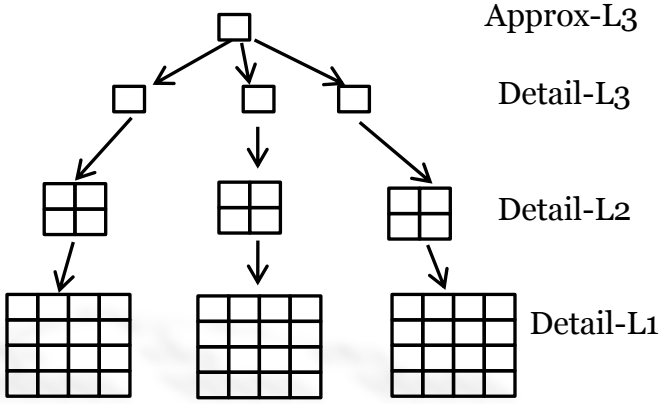

Figure3.3 Wavelet coefficient tree based on parent-child dependency for a three-level decomposition

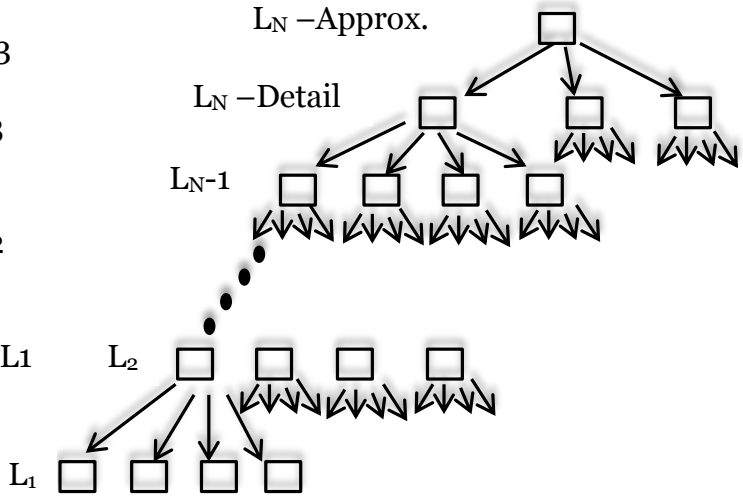

Figure3.4 Generalized wavelet coefficient tree based on parent-child dependency for N-level decomposition

Figure 3.3 depicts the parent-child dependency of wavelet subband diagram shown in figure 3.1 in tree formation. Figure 3.4 depicts the generalized tree formation for any arbitrary N-level decomposition. After the Nth level detail each pixel node is associated with four pixels down the level. This is demonstrated with the help of arrows shown in the figure 3.4.

3.4 Concept of Zero-Tree in EZW

The wavelet transform tree for decomposition coefficients has been discussed above with respect to parent-child dependencies. *If the root of wavelet coefficient tree and all its corresponding descendants are less than the given threshold then the tree is said to be Zero-tree* and the *corresponding root is said to be Zero-tree root (ZTR).* This is applicable to the roots and trees at all decomposition levels, while the whole image decomposition subband is being traversed according to the scanning order. The root of zero-tree is used to represent the whole tree in EZW. The zero-tree root can be encoded in the Dominant with some zero-tree symbol say, 'ZTR' and while decoding in the Subordinate pass zero value is placed at the zero-tree root and at its corresponding descendants nodes. Thus the whole tree is encoded in a single symbol of 'ZTR'.

As we can see from figure 3.1, which is the "Cameraman" image's wavelet decomposition up to three levels, that most of the image subband is dark. This means that many coefficients are near to zero except for the regions where edges occur. Thus, while encoding an image using EZW a large number of zero-trees are encountered. This particular aspect of wavelet based image decomposition in subbands improves the efficiency of the coding and results in much improved compression ratio.

3.5 Concept of Isolated-Zero in EZW

If the root of the wavelet coefficient tree at any level *is less than the given threshold but one or some of its descendant are greater than the given threshold, then the root is said be an Isolated Zero.* It is important to note that, only the root and not the entire tree is encoded in case of isolated zero in EZW.

3.6 Concept of Positive and Negative Significant in EZW

If the *absolute value of the coefficient* in the wavelet subband decomposition of image *is greater than the given threshold then the coefficient value is termed as a Significant.* Correspondingly, *if the sign of the coefficient is positive*, it is termed as *positive significant* and if it is *negative* it is termed as *negative significant*. The positive and negative significant bits in the significance map are the information carrying bits; and the rest are zeros.

3.7 Embedded Zero-tree Wavelet Coding Algorithm

The embedded zero-tree wavelet coding mainly consist of two passes – Dominant Pass and the Subordinate Pass.

Firstly, discrete wavelet transform is applied upon the image and the wavelet subband decomposition of the image is obtained up to the desired level. The example of wavelet subband of an image is shown in figure 3.1.

The EZW algorithm is an iterative algorithm. Each pass produces more detailed information of the image. First the initial threshold is fixed and the Dominant pass is applied over the wavelet subbands. The result of Dominant pass is passed to the Subordinate pass. A bit stream is generated at the output which is related to the given threshold. For the next iteration or EZW loop the threshold is lowered, generally by a factor of 2 and again the process is repeated. This results in higher bit rate and embedded bit stream. The algorithm is repeated iteratively up till a desired number of passes or a specific bitrate or up till the bit budget is exhausted.

3.7.1 Dominant Pass (Significance Map Pass)

In the Dominant pass the coefficients are tested for their significance. If the absolute value of wavelet coefficient *x* is greater than the given threshold *T*, i.e. $|x| > T$ then the coefficient is said to be significant. Accordingly there are positive and negative significant as explained in section 3.4.

The Dominant Pass mainly checks the wavelet coefficient for the Positive significant (P), Negative significant (N), Zero-tree root (ZTR) and Isolated Zero (IZ) and encodes a symbol for it accordingly. The scan should be in such manner that no child should be scan before its parent. Figure 3.5 shows the flowchart for scanning the wavelet coefficients in the dominant pass.

The EZW maintains two lists; Dominant list and Subordinate list. The one concerned with this pass is *Dominant List*. In the dominant list initially the *coordinates* of the entire coefficients are placed. In the successive passes the coefficients found significant are removed from the list and

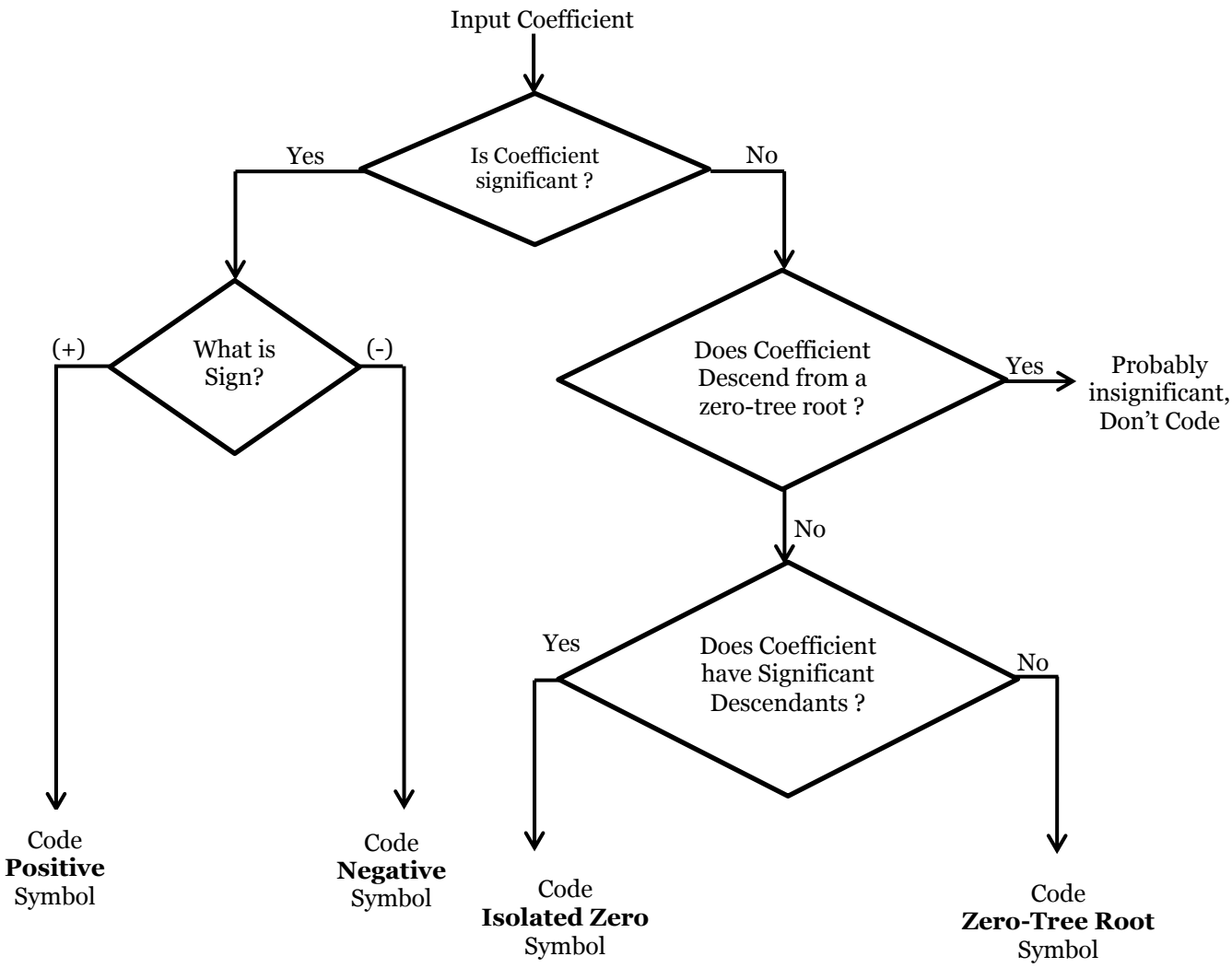

Figure3.5 Flowchart for Encoding of Significant, Isolated zero and Zero-tree root coefficients in the Dominant pass of EZW

their *magnitudes* are placed on the subordinate list. Thereafter, the significant coefficient in the wavelet transform array is replaced by zero so that it does not prevent the occurrence of a zero-tree in future dominant passes at smaller thresholds. Thus the dominant list contains the coordinates of those coefficients that have not yet been found to be significant, in the same relative order as the initial scan.

At the completion of Dominant pass a bit stream of symbols is generated. After each pass the current threshold is divided by a factor of two. Now for next iterative pass the value of threshold is decreased, thus the number of significant coefficients increases and accordingly the bit stream

carries more image information now. Thus as the number of pass increases the dominant list starts to decrease and the subordinate list starts to increase.

The coefficients once encoded as significant in the map, remain significant for all passes, though their decoding value changes due to quantization in the subordinate passes. When other coefficients are found significant their coordinates too are encoded in the map with the corresponding symbol. Thus in this way the bit stream is appended and updated in each iterative pass. This results in an embedded bit stream.

3.7.2 Subordinate Pass (Significance Coefficient Refinement Pass)

Dominant pass is followed by the Subordinate Pass. In each iterative pass of EZW after the Dominant pass the corresponding Subordinate pass is called. The current Subordinate List and the symbol bit stream are processed by the subordinate pass.

On the *Subordinate List* the *magnitude* of the coefficients are placed which are found to be significant in the dominant pass. Thus the subordinate list consists of significant coefficient values with sign. The subordinate pass in every iterative pass, refines the range in which the significant coefficients lie. Thus it is also called as refinement pass.

For the first dominant pass the initial threshold is half of the maximum absolute value of the coefficient value in the wavelet transform subband. So if the wavelet transform subband array is denoted by L then the maximum absolute coefficient value L_{max} can be taken as,

$$L_{max} = max([\,|L|\,]) \tag{3.1}$$

Thus the maximum initial threshold T_1 comes out to be,

$$T_1 = integer\ (L_{max}/2) \tag{3.2}$$

In the first pass the threshold is T_1 i.e. half of L_{max}, as stated before. Thus it can be observed that, all coefficients which turn out to be significant i.e. $|x| > T_1$ during first dominant, pass have absolute values lying in the range of $\boldsymbol{(T_1,\ L_{max}]}$, since L_{max} is the maximum value that a coefficient can have is L_{max}.

In the subordinate pass this range of (T_1, L_{max}] is refined. The subordinate pass performs pixel value quantization which achieves compression by telling the decoder with a symbol roughly what the pixel value is, instead of exactly what the pixel value is. The range in the each pass is divided into two parts – the upper half and the lower half. This means that the range of (T_1, L_{max}] is broken into **(T_1, $3T_1/2$]** and **($3T_1/2$, L_{max}]**. On the encoding side, the significant coefficient value lying in the upper half are encoded with a symbol of "1" and those significance lying in the lower half range are encoded with the symbol of "0".

On the decoding side, the decoder roughly generates the coefficient value using approximation. The coefficients lying in the corresponding range are assigned the mean value of the corresponding range. Thus, in the above stated case the values in the upper range area assigned the mean value $5T_1/4$ and the values of upper half are assigned $7T_1/4$. Next, the sign to the assigned value is given according to its positive or negative significance.

In the next pass, the threshold is reduced by a factor of two. Thus $T_2=T_1/2$. Now, the already divider range of the previous pass becomes the range for the current dominant pass with one more interval added to it, ($T_2=T_1/2$, T_1], due to lowering of threshold (For simplicity T_2 has been replaced by $T_1/2$). It is interesting to note that all the three intervals for dominant pass **($T_1/2$, T_1]**, **(T_1, $3T_1/2$]** and **($3T_1/2$, L_{max}]** are equally spaced. This is due to division by a factor of two each time both in threshold and in coefficient range.

These current dominant range intervals are now divided in to lower and upper halves. Thus, the obtained subordinate intervals are **($T_1/2$, $3T_1/4$]**, **($3T_1/4$, T_1]**, **(T_1, $5T_1/4$]**, **($5T_1/4$, $3T_1/2$]**, **($3T_1/2$, $7T_1/4$]**, **($7T_1/4$, L_{max}]**. While decoding the significant encoded value lying in these intervals are assigned the mean value of the corresponding interval, in which they occur. Thus the values assigned correspondingly are $5\ T_1/8$, $7T_1/8$, $7T_1/8$, $9T_1/8$, $11T_1/8$, $13T_1/8$ and $15T_1/8$. Next, the sign to the assigned value is given according to its positive or negative significance.

This same process is repeated in all iterative subordinate passes of EZW. It is an interesting thing to know that the intervals in the successive subordinate pass are twice than in previous pass plus two. This rough approximation and quantization is termed as Successive-Approximation Entropy-Coded Quantization in EZW literature.

Though the encoded image is quantized as stated above, yet the decoded image for higher passes of the EZW have high PSNR as in the successive passes the number of encoding intervals increases and also the interval length is reduced by half each time. Thus assigned mean value is coming closer to the real coefficient value. Yet, the decoded image is formed with much less energy and less number of significant coefficients; majority are still zeros.

3.8 Chapter Summary

The chapter gives detailed information about Embedded Zero Tree Wavelet Encoding which was discussed and given by Shapiro. The parent-child dependency in wavelet transform subband is the base of EZW. The coding mainly revolves around dominant and subordinate pass in which first the map of significance coefficients is encoded and then they are assigned a quantized value through approximation. EZW produces an embedded bit stream and the encoding is stopped when the bit budget is exhausted.

Chapter 4

Improved EZW on the basis of Descendant Scanning

4.1 Introduction to the Improving Concept

In the each pass of embedded zero-tree wavelet coding each coefficient is scanned for positive or negative significance, isolated zero and zero-tree root. This is done in each iterative pass of the algorithm. The major execution time in the dominant pass of the algorithm is consumed in scanning the tree of insignificant coefficients for zero-tree or insignificant zeros.

It has been shown that most of the detail subbands are dark at all the levels in the decomposed subband structure. This clearly means that most of the coefficient values in the detail subband are near to zero. Thus even in successive iterative passes, where the threshold is reduced each time by a factor of 2, they may not become significant; as they are near to zero.

Thus a significant improvement in the execution time of the existing algorithm can be made, if the descendants of zero-trees of the previous passes are not scanned in successive passes considering that most of these values are near to zero and will not become significant at all during the successive passes even when the threshold value is low. The descendants are chosen because they will always lie in the detail subband, where as a zero-tree root may also lie in the approximation subband.

The above stated concept forms the base of the proposed work. In the proposed work a few algorithms have been derived by altering the dominant pass of EZW and then at the last the best of them is proposed as improved algorithm; mainly on the basis improved execution time and peak signal to noise ratio at the same iterations.

4.2 Coding Scheme *A*

The coding scheme *A* is based on the previously stated concept for execution time improvement in wavelet zero-trees. The changes are made in the dominant pass of the algorithm and the subordinate pass in which approximation and quantization are done, remains the same. The algorithm can be explained with the help of flowchart shown in figure 4.1

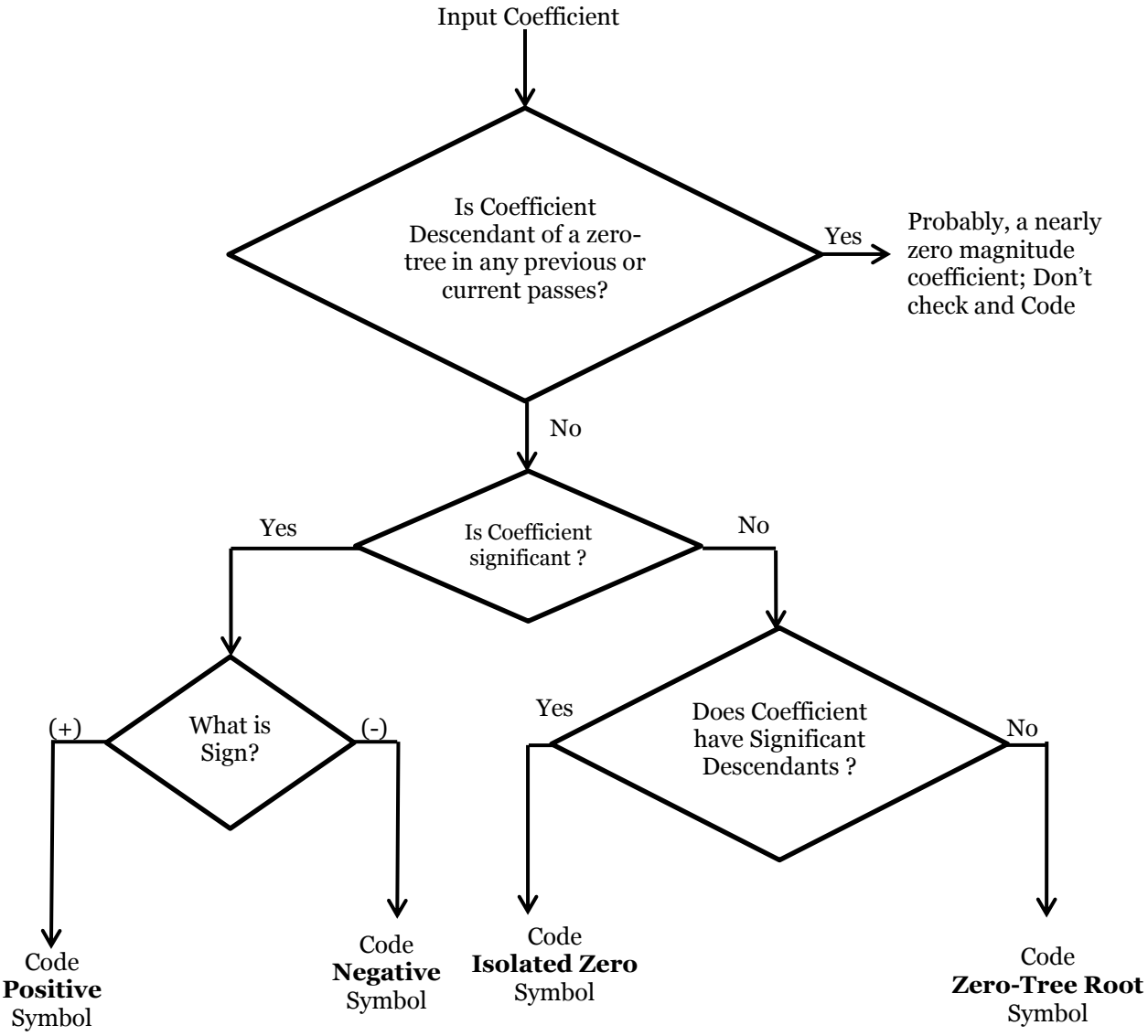

Figure 4.1 Coding Scheme *A*

4.2.1 Advantages and Drawbacks

The first and the foremost advantage of the Coding Scheme *A* is that the execution time of the algorithm in the dominant pass improves greatly. This is due to ignorance of coefficients which become descendants of zero-trees in any iterative pass. Only for the first iterative pass whole of the decomposition subband is scanned. Since large numbers of zero-trees are encountered, there are large numbers of descendants. These descendants are not scanned again in the next passes assuming that they have almost zero magnitude. Thus the execution time improves.

The detail subbands in the wavelet decomposition subband contains edges which can have coefficient magnitude much greater than zero. In the initial passes the threshold is high and the edges and other details having coefficient values less than the encoding threshold may come under the descendants of zero-tree roots. Thus they will not be scanned again in any of the successive passes and will not become significant even if the threshold is lowered down enough. Thus the particular coding scheme improves the execution time on the compromise of loosing some details.

Thus, another stricter coding scheme is brought out which does not compromise on quality of the uncompressed image.

4.3 Coding Scheme *B*

Coding scheme *B* is also a derivative of embedded zero-tree wavelet encoding technique which is also not much different from it. In this coding scheme the descendants and zero-tree roots of the previous passes are checked and evaluated for significance, the restriction is made only on the descendants of the current pass. The coding scheme *B* is does not improve the execution time much but it does not compromise on the quality of uncompressed image. The scheme is based on checking the coefficient for being descendant of a zero-tree before checking the coefficient for its significance which has already been done previously while scanning for the zero tree root. Thus all the descendants are not checked for being significant as in case of EZW. This saves some of the time. The coding scheme is illustrated in figure 4.2.

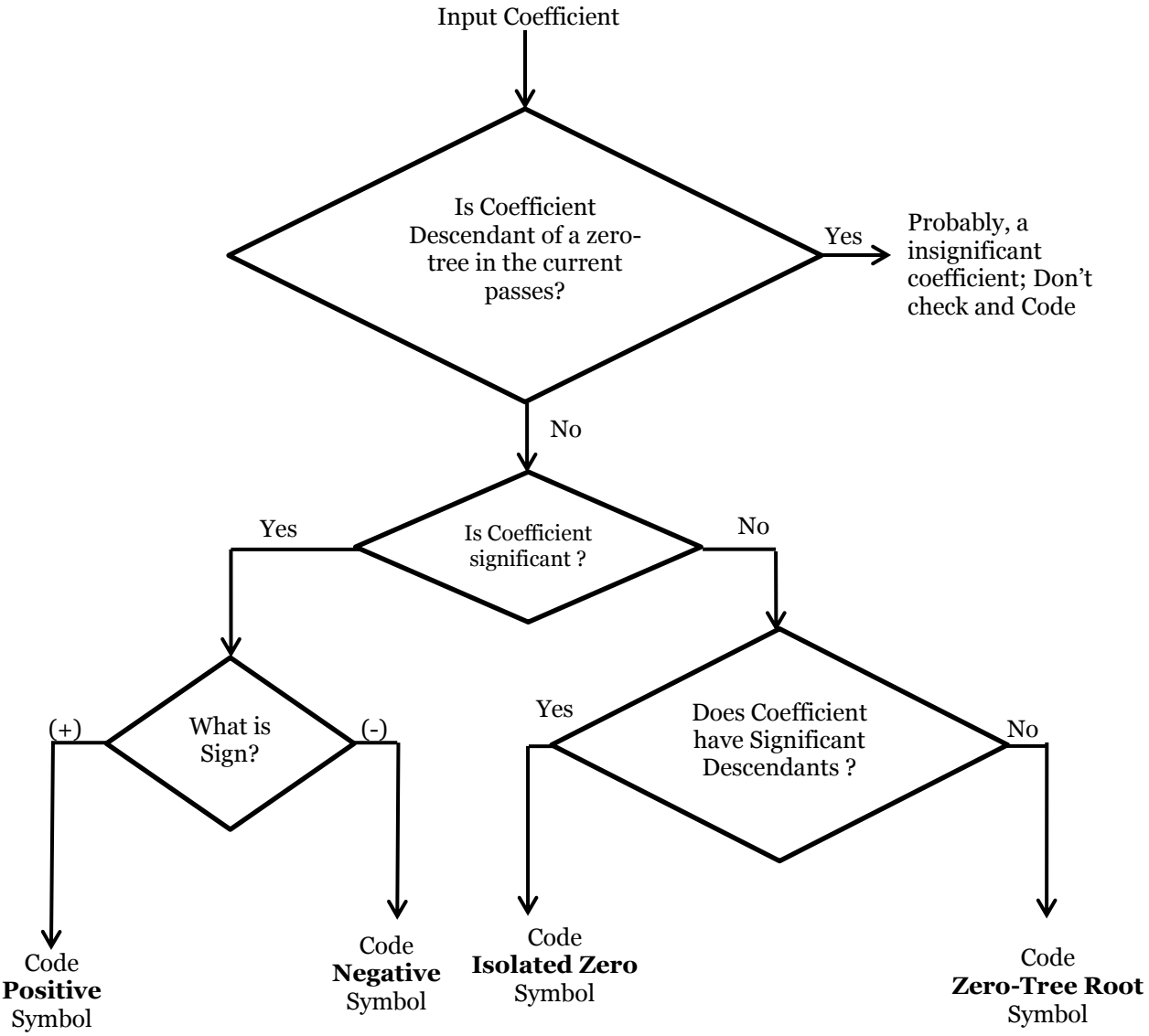

Figure 4.2 Coding Scheme *B*

4.3.1 Advantage and Drawbacks

The advantage is that the quality of image is maintained even after compression but the drawback is that there is not much improvement in the execution time of the dominant pass.

4.4 *Proposed* Coding Scheme *C*

The Coding Scheme *C* incorporates the effect and advantages of both the algorithms *A* and *B*. In Coding Scheme *C* first the restriction is not applied on the descendant of previous passes. This

ensures that the edge and detail information in the detail subbands is encoded and their coefficients become significant. Thus they are brought out descendants in successive passes by lowering the threshold and checking them for their significance and encoding them if found so.

After a certain reach it is believed that the coefficients containing information about the edges are no more descendants of zero-tree but have been encoded as significant. It is now assumed that the majority of the wavelet zero-trees contain descendants which have magnitudes near to zero and will not become significant in further passes and also from here the remaining edges and details will be accounted by Isolated Zeros which may become significant in the further passes.

This is implemented by combining the two previous algorithms in correct manner. Up till a certain pass the stricter coding scheme *B* is executed and after that when it is believed that the majority of the wavelet zero-trees are carrying descendants which have magnitudes nearly zero coding scheme *A* is applied, in which scanning of the descendants of previous passes is skipped in successive passes.

The iterative pass at which the coding scheme are changed is termed here as *detail retaining pass*. Thus coding scheme *C* provides solution for problem arising in coding scheme *A*. through coding scheme *B*. The scheme *C* is illustrated with the help of flowchart figure 4.3.

By selecting the edge retaining pass carefully suitable changes can be made in the output according to user in which execution time and quality of uncompressed image both are taken care of.

4.4.1 Advantages

The coding scheme *C* is a unique and efficient way to encode the image differently in the dominant pass by defining the *Detail Retaining Pass (DRP) number*. In a way a threshold is being fixed above which the edge coefficient exist. The symbols kept for encoding the different properties of the subband (P, N, IZ, ZTR) are same at the end of both the sub-branches. Thus there is no extra coding cost incurred due to increase of symbol. This also allows keeping the subordinate pass unaltered and it is formulated in the same manner as in EZW coding. The

coding algorithm *C* is a better way to encode image in lesser time. In this suitable changes can be brought about by varying the Detail Retaining Pass number.

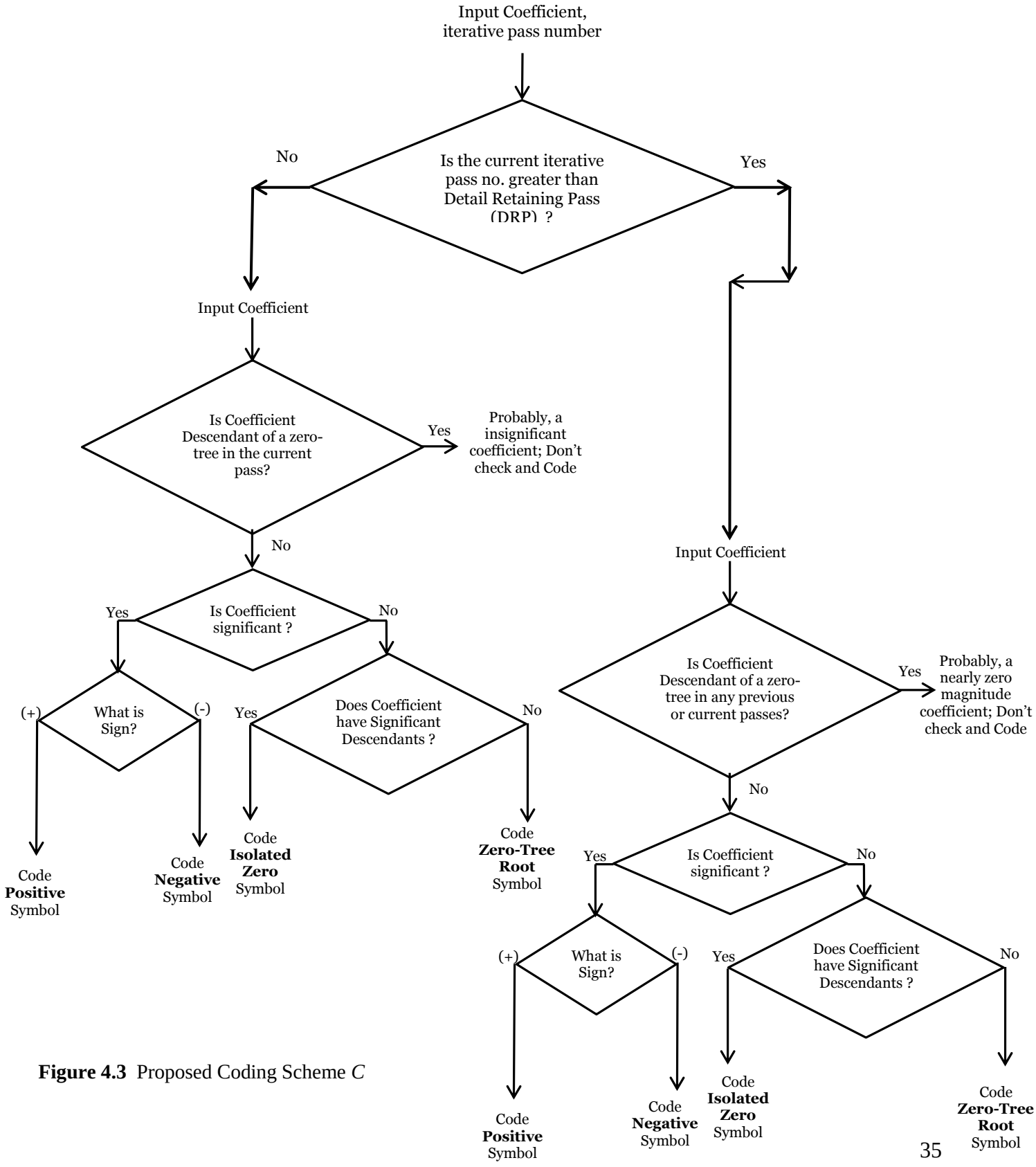

Figure 4.3 Proposed Coding Scheme *C*

Chapter 5

Results and Discussion

5.1 Implementation

The functions for the code for EZW and the proposed coding were written in MATLAB. Various functions for implementing different steps of the algorithm were made. The steps with respect to functions made are mentioned below.

1. Obtain Discrete Wavelet transform of the Test Image using a defined wavelet.
    i. Function for arranging the 1-D array of wavelet coefficients into 2-D Subband.
2. Dominant Pass function – according to different schemes.
    i. Test for positive and negative significance. Tree scanning function for insignificant node according to the subband in which it lies.
    ii. Function to determine if the node is zero-tree root or isolated zero.
3. Subordinate pass function for quantization
4. Arrange quantized coefficients according to subbands.
5. Obtain Inverse Discrete Wavelet Transform using a defined wavelet.
6. Obtain image and calculate various parameters.

5.2 Parameters for performance measurement

(a) Encoding Time

It is the time used to encode the original image using image compression encoded algorithm. It is measured in seconds.

(b) Decoding Time

It is the time used to decode the encoded image by using the decoding algorithm in order to obtain the decompressed image. It is measured in seconds.

(c) Mean Square Error (MSE)

Mean square error (MSE) is the cumulative squared error obtained between original and recovered image.

$$MSE = \frac{1}{mn} \sum_{i=0}^{m-1} \sum_{j-0}^{n-1} \|I(i,j) - K(i,j)\|^2 \quad (5.1)$$

Larger the value of MSE means poorer is the quality of image

(d) Peak Signal to Noise Ratio (PSNR)

For a lossy compression algorithm, a distortion measurement is used to measure how much information has been lost when a reconstructed version of a digital image is produced from the compressed data. The PSNR is used to measure the performance of lossy compression algorithms. So, it defines the ratio between the maximum possible power of a signal and the power of corrupting noise that affects the fidelity of its representation. Because many signals have a very wide dynamic range, PSNR is usually expressed in terms of the logarithmic decibel scale.

The PSNR is most commonly used as a measure of quality of reconstruction of lossy compression.

$$PSNR = 10\ log_{10}\left(\frac{MAX_i^2}{MSE}\right) \quad (5.2)$$

$$= 20\ log_{10}\left(\frac{MAX_i}{\sqrt{MSE}}\right) \quad (5.3)$$

Here, MAX_i is the maximum possible pixel value of the image. Generally for unsigned 8-bit gray scale image it is 255.

Small value of PSNR means poor quality image. PSNR is very fast and easy to implement.

(e) Compression Ratio

Compression efficiency is measured by compression ratio, which is defined as the rate of the size (number of bits) of the original image data over the size of the compressed image data.

$$C_R = \frac{n_1}{n_2} \tag{5.4}$$

Where, C_R is the compression ratio, n_1 and n_2 is the number of information carrying units in the original and encoded images respectively. In case of transform coding, such as wavelet transforms where the transform coefficients are saved or transmitted the compression ratio is determined by calculating the difference between the coded coefficient and the total number of coefficients and then dividing it by the total number of coefficients.

(f) Bit per pixel

Bit per pixel (bpp) of the image is the number of bits of information stored per pixel of an image. A gray scale image having gray levels from 0 to 255 is an 8 bit per pixel image. In case of decoded image bpp can be calculated by obtaining the total number of bits i.e. number of significant coefficients multiplied by 8 and then dividing them by total number of pixels (or total number of coefficients).

5.3 Results

Results have been obtained on MATLAB, installed on Windows XP based operating system with 1 GB RAM, Intel Core2 Duo 2.10Ghz Processor and 240GB HDD.

While obtaining results for the execution time it was tried to keep the conditions constant all the time. And it was tried to reduce the execution of parallel processes. Thus internet connection was disabled and all other applications were closed. Results have been obtained on various test

images. In all the test images, for wavelet decomposition and reconstruction Biorthogonal 4.4 wavelet was used and the decomposition was done up to three levels.

5.3.1 Results on test image1 – Elaine

Grayscale image of Elaine of Size 512 x 512 was taken as the first test image.

Figure 5.1 Test Image1-'Elaine'

5.3.1(a) Coding Scheme A

The Coding Scheme A was applied over the Elaine image for 10 passes and various parameters were recorded including the execution time of the dominant pass.

The total execution time in sec. of 10 Dominant passes, without estimating subordinate pass time, is 43.1118 sec. The results of various parameters over 10 passes are shown in table-I.

Table-I: Parameter of Coding Scheme A on Elaine Image

Test Img. Elaine/thr.	1 Thr=960	2 Thr=480	3 Thr=240	4 Thr=120	5 Thr=60	6 Thr=30	7 Thr=15	8 Thr=8	9 Thr=4	10 Thr=2
Execution Time(sec.)	17.1241	3.2168	3.1676	3.1634	3.5030	3.0887	2.9913	2.7134	2.2358	1.8675
PSNR(dB)	7.2513	14.4383	21.2881	23.9051	25.4800	27.9196	28.2555	28.5446	28.7604	28.8338
MSE	1.22e+004	2.34e+003	483.356	264.5881	184.1107	104.9837	97.1695	90.9121	86.5051	85.0542
bpp	1.0112	1.0516	1.0560	1.0599	1.0755	1.1128	1.2108	1.5932	2.4393	3.2852
CR %	87.3596	86.8546	86.8004	86.7512	86.5562	86.0905	84.8648	80.0846	69.5087	58.9348

The decoded images at the end of passes 3 to 8 are shown in figure 5.2.

(a) Thr=240, PSNR=21.2881 (b) Thr=120, PSNR=23.9051 (c) Thr=60, PSNR=25.4800

(d) Thr=30, PSNR=27.9196 (e) Thr=15, PSNR=28.2555 (f) Thr=8, PSNR=28.5446

Figure 5.2(a)-(f) Decoded Images of passes 3 to 8 of Coding Scheme A

5.3.1(b) Coding Scheme B

The Coding Scheme B was applied over the Elaine image for 10 passes and various parameters were recorded including the execution time of the dominant pass.

The total execution time in sec. of 10 Dominant passes, without estimating subordinate pass time, is 55.1864 sec. The results of various parameters over 10 passes are shown in table-II.

Table-II: Parameter of Coding Scheme B on Elaine Image

Test Img. Elaine/thr.	1 Thr=960	2 Thr=480	3 Thr=240	4 Thr=120	5 Thr=60	6 Thr=30	7 Thr=15	8 Thr=8	9 Thr=4	10 Thr=2
Execution Time(sec.)	16.8366	4.2679	4.3558	4.3844	5.2037	4.4002	4.6457	4.4458	3.6317	2.8990
PSNR(dB)	7.2513	14.4383	21.2922	24.1579	26.1898	29.8013	30.9520	32.5003	35.1893	35.9902
MSE	1.2245e+04	2.3402e+03	482.9027	249.6250	156.3519	68.0694	52.2250	31.9191	19.6855	16.3706
bpp	1.0112	1.4557	1.5000	1.5016	1.5171	1.5672	1.9686	3.0542	4.6774	6.0726
CR %	87.3596	81.8039	81.2500	81.2302	81.0360	80.4108	75.3914	61.8214	41.5337	24.0921

The decoded images at the end of passes 6 to 8 are shown in figure 5.3.

(a) Thr=30, PSNR=29.8013 (b) Thr=15, PSNR=30.9520 (c) Thr=8, PSNR=32.5003

Figure 5.3(a)-(f) Decoded Images of passes 6 to 8 of Coding Scheme B

5.3.1(c) Proposed Coding Scheme C

The Coding Scheme C was applied over the Elaine image for 10 passes and various parameters were recorded included the execution time by setting Detail Retaining Pass Number different each time.

(i) Detail Retaining Pass Number (DRP) = 3

The total execution time in sec. of 10 Dominant passes, without estimating subordinate pass time, is 52.6180 sec. The results of various parameters over 10 passes are shown in table-III.

Table-III: Parameter of Coding Scheme C with DRP=3 on Elaine Image

Test Img. Elaine/thr.	1 Thr=960	2 Thr=480	3 Thr=240	4 Thr=120	5 Thr=60	6 Thr=30	7 Thr=15	8 Thr=8	9 Thr=4	10 Thr=2
Execution Time(sec.)	17.5678	4.3123	4.4288	4.3960	4.9680	4.2653	4.0135	3.5371	2.7970	2.2893
PSNR(dB)	7.2513	14.4383	21.2922	24.1579	26.1898	29.7711	30.7130	31.8102	32.6802	32.9721
MSE	1.2245e+004	2.3402e+003	482.9027	249.6250	156.3519	68.5447	55.1800	42.8610	35.0800	32.7997
bpp	1.0112	1.4557	1.5000	1.5076	1.5360	1.6028	1.8145	2.5700	3.9665	5.2042
CR %	87.3596	81.8039	81.2500	81.1550	80.8002	79.9656	77.3193	67.8745	50.4189	34.9476

The decoded images at the end of passes 6, 7 and 8 are shown in figure 5.4.

(a) Thr=30, PSNR=29.7711 (b) Thr=15, PSNR=30.7130 (c) Thr=8, PSNR=31.8102

Figure 5.4(a)-(c) Decoded Images of passes 6 to 8 of Coding Scheme C with DRP=3

(ii) Detail Retaiaing Pass = 4

The total execution time in sec. of 10 Dominant passes, without estimating subordinate pass time, is 53.5754 sec. The results of various parameters over 10 passes are shown in Table-IV.

Table-IV: Parameter of Coding Scheme C with DRP=4 on Elaine Image

Test Img. Elaine/thr.	1 Thr=960	2 Thr=480	3 Thr=240	4 Thr=120	5 Thr=60	6 Thr=30	7 Thr=15	8 Thr=8	9 Thr=4	10 Thr=2
Execution Time(sec.)	18.5772	4.2689	4.3845	4.4245	4.9598	4.2641	4.0181	3.5391	2.8192	2.2766
PSNR(dB)	7.2513	14.4383	21.2922	24.1579	26.1898	29.7789	30.7271	31.8285	32.7022	32.9957
MSE	1.2245e+004	2.3402e+003	482.9027	249.6250	156.3519	68.4208	55.0010	42.6803	34.9028	32.6221
bpp	1.0112	1.4557	1.5000	1.5016	1.5300	1.5971	1.8094	2.5652	3.9620	5.1997
CR %	87.3596	81.8039	81.2500	81.2302	80.8746	80.0358	77.3823	67.9352	50.4753	35.0040

The decoded images at the end of passes 6, 7 and 8 are shown in figure 5.5.

(a) Thr=30, PSNR=29.7789 (b) Thr=15, PSNR=30.7271 (c) Thr=8, PSNR=31.8285

Figure 5.5(a)-(c) Decoded Images of passes 6 to 8 of Coding Scheme C with DRP=4

(iii) Detail Retaiaing Pass = 5

The total execution time in sec. of 10 successive Dominant passes, without estimating subordinate pass time, is 53.4396 sec. The results of various parameters over 10 passes are shown in Table-V.

Table-V: Parameter of Coding Scheme C with DRP=5 on Elaine Image

Test Img. Elaine/thr.	1 Thr=960	2 Thr=480	3 Thr=240	4 Thr=120	5 Thr=60	6 Thr=30	7 Thr=15	8 Thr=8	9 Thr=4	10 Thr=2
Execution Time(sec.)	17.8318	4.2955	4.4004	4.3692	5.3523	4.3086	4.0851	3.6262	2.8363	2.3055
PSNR(dB)	7.2513	14.4383	21.2922	24.1579	26.1898	29.7789	30.7271	31.8285	32.7022	32.9957
MSE	1.2245e+004	2.3402e+003	482.9027	249.6250	156.3519	68.4208	55.0010	42.6803	34.9028	32.6221
bpp	1.0112	1.4557	1.5000	1.5016	1.5300	1.5971	1.8094	2.5652	3.9620	5.1997
CR %	87.3596	81.8039	81.2500	81.2302	80.8746	80.0358	77.3823	67.9352	50.4753	35.0040

The decoded images at the end of passes 6, 7 and 8 are shown in figure 5.6.

(a) Thr=30, PSNR=29.7789 (b) Thr=15, PSNR=30.7271 (c) Thr=8, PSNR=31.8285

Figure 5.6(a)-(c) Decoded Images of passes 6 to 8 of Coding Scheme C with DRP=5

5.3.1(d) Discussion It can be seen from the results brought out in previous section that the proposed algorithm C works well with respect to the approximation that was stated in chapter 4. The time of execution of Dominant Pass uptill various numbers of iterative passes has been recorded in Table-VI.

Table-VI: Execution Time of Dominant Passes recorded uptill different iterative passes in sec.

Scheme →	A	B	C, DRP=3	C, DRP=4	C, DRP=5
Pass 6	33.7409	40.5658	39.7169	39.1332	40.0930
Pass 7	36.2469	44.3869	43.4898	43.1651	43.4938
Pass 8	39.2764	49.3653	46.8478	46.6394	47.2291
Pass 9	41.2346	52.4209	49.5443	49.6182	50.7646
Pass 10	43.1118	55.1864	52.6180	53.5754	53.4396

The PSNR of Elaine image obtained after decoding at subordinate pass of different algorithms has been plotted in figure 5.7 for different iterative passes.

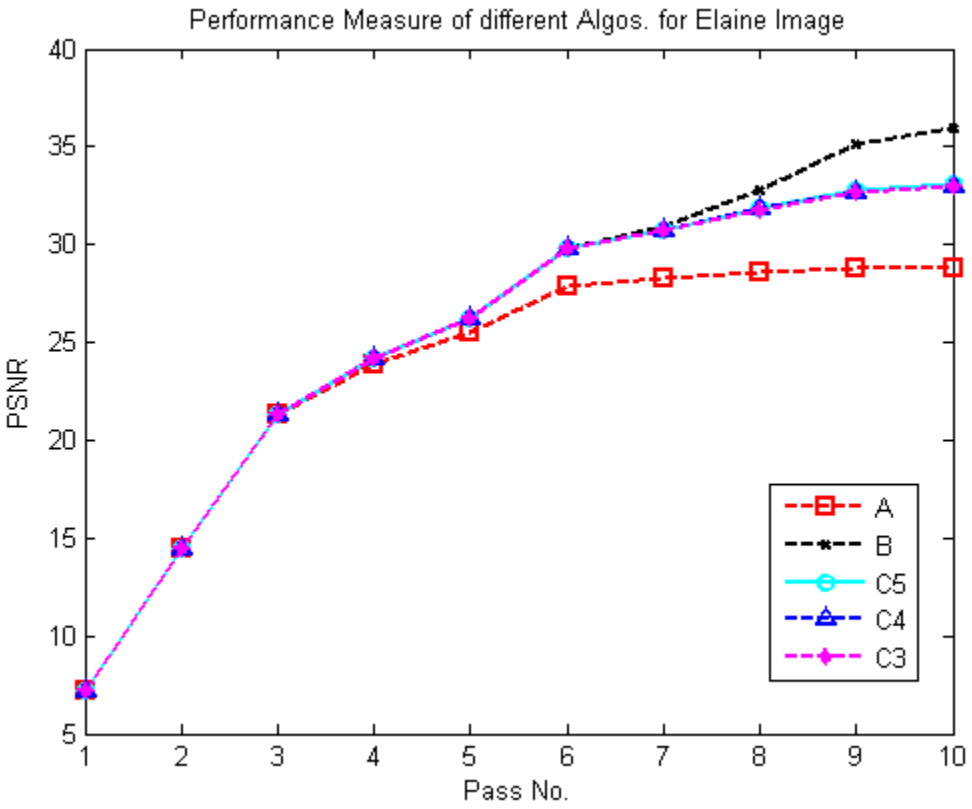

Figure 5.7 PSNR plot of uncompressed decoded Elaine Image at different iterative passes

It can be clearly seen from Table-VI that there is a difference of fractions of second for total of 6 iterative dominant passes in algorithm B and C with Drp=3. Algorithm B is logically same as EZW. In 7 successive dominant pass iterations the difference becomes almost 2 second. In 8 passes the difference is almost 3 seconds and is maintained so thereafter in more number of passes.

It can be seen from figure 5.7 that PSNR values of Algorithm C for different value of Detail Retaining Pass (Drp) are almost same. But from Table-VI it can be seen that algorithm C with Drp=3 takes least time to execute among them. Coding Scheme A executes quickest but has low PSNR values after 4 successive dominant pass iterations. Also it can be seen that algorithm C with different Drp have same PSNR values uptill 7 iterative passes. Thus the improvement of 2 seconds have been made by coding scheme C with Drp=3 in EZW up till 7 iterative passes. It can also be seen form Table-II and Table-III that the compression ratio has also been improved

by 2%, from 75.39% to 77.31% and the bit per pixel has also been reduced by 0.1, in the result of 7^{th} iterative pass.

It can be seen from Table-II, Table-III and Table-IV that at the end of 8^{th} iterative pass improvement of 3 sec. can be made if a fall of 1dB is allowed in PSNR. The threshold in the 8^{th}, 9^{th} and 10^{th} iterative pass is very low. It is 8, 4 and 2 correspondingly; which is much close to zero as compared with initial threshold of 960 for the 1^{st} dominant pass. Thus the approximation that the descendants of zero-tree roots are nearly zero valued becomes null as the variation in coefficient appear when the threshold becomes so low. Hence for passes 9 and 10, coding scheme B is better and the PSNR is higher by 3db as compared to coding scheme C.

5.3.2 Results on test image2 – Pirate

The Grayscale Pirate image of Size 512 x 512 was taken as the second test image.

Figure 5.8 Test Image2-'Pirate'

5.3.2(a) Coding Scheme A

The Coding Scheme A was applied over the Pirate image for 10 passes and various parameters were recorded including the execution time of the dominant pass.

The total execution time in sec. of 10 Dominant passes, without estimating subordinate pass time, is 39.4757 sec. The results of various parameters over 10 passes are shown in table-VII.

Table-VII: Parameter of Coding Scheme A on Pirate Image

Test Img. Pirate/thr.	1 Thr=871	2 Thr=436	3 Thr=218	4 Thr=109	5 Thr=54	6 Thr=27	7 Thr=14	8 Thr=7	9 Thr=3	10 Thr=2
Execution Time(sec.)	14.9090	2.9067	2.8643	2.8530	3.8889	3.9850	2.4175	2.1175	1.8430	1.6513
PSNR(dB)	9.2500	16.3790	21.9424	23.6980	24.8602	25.9600	26.4937	26.7451	26.8373	26.8655
MSE	7.7282e+3	1.4969e+3	415.7548	277.5080	212.3546	164.8478	145.7830	137.5858	134.6951	133.8233
bpp	0.8857	0.9232	0.9427	0.9544	1.0003	1.1317	1.3796	1.8003	2.5202	2.8823
CR %	88.9290	88.4602	88.2164	88.0703	87.4958	85.8540	82.7553	77.4963	68.4975	63.9709

The decoded images at the end of passes 6 to 8 are shown in figure 5.9

(a) Thr=27, PSNR=25.9600 (b) Thr=14, PSNR=26.4937 (c) Thr=7, PSNR=26.7451

Figure 5.9(a)-(c) Decoded Images of passes 6 to 8 of Coding Scheme A

5.3.2(b) Coding Scheme B

The Coding Scheme B was applied over the Pirate image for 10 passes and various parameters were recorded including the execution time of the dominant pass.

The total execution time in sec. of 10 Dominant passes, without estimating subordinate pass time, is 55.0811 sec. The results of various parameters over 10 passes are shown in table-VIII.

Table-VIII: Parameter of Coding Scheme B on Pirate Image

Test Img. Pirate/thr.	1 Thr=871	2 Thr=436	3 Thr=218	4 Thr=109	5 Thr=54	6 Thr=27	7 Thr=14	8 Thr=7	9 Thr=3	10 Thr=2
Execution Time(sec.)	14.8319	3.9127	4.4191	4.4288	8.8618	4.3257	4.1332	3.7660	3.2756	3.0082
PSNR(dB)	9.2500	16.3790	21.9705	24.2088	26.3402	29.3354	31.8982	34.6317	36.1336	36.8083
MSE	7.7282e+003	1.4969e+003	413.0728	246.7156	151.0291	75.7778	39.1976	22.3824	15.8387	13.5597
bpp	0.5386	1.2982	1.5000	1.5068`	1.5566	1.7386	2.1056	2.7935	4.2022	5.0479
CR %	93.2678	83.7719	81.2500	81.1646	80.5424	78.2669	73.6801	65.0818	47.4724	36.9015

The decoded images at the end of passes 6 to 8 are shown in figure 5.10

(a) Thr=27, PSNR=29.3354 (b) Thr=14, PSNR=31.8982 (c) Thr=7, PSNR=34.6317

Figure 5.10(a)-(c) Decoded Images of passes 6 to 8 of Coding Scheme B

5.3.2(c) Proposed Coding Scheme C

The Coding Scheme C was applied over the Pirate image for 10 passes and various parameters were recorded included the execution time by setting Detail Retaining Pass Number different each time.

(i) Detail Retaining Pass Number (DRP) = 3

The total execution time in sec. of 10 Dominant passes, without estimating subordinate pass time, is 51.4581 sec. The results of various parameters over 10 passes are shown in table-IX.

Table-IX: Parameter of Coding Scheme C with DRP=3 on Pirate Image

Test Img. Pirate/thr.	1 Thr=871	2 Thr=436	3 Thr=218	4 Thr=109	5 Thr=54	6 Thr=27	7 Thr=14	8 Thr=7	9 Thr=3	10 Thr=2
Execution Time(sec.)	14.8496	3.8770	4.3635	4.3381	6.8139	5.5997	3.6121	3.0873	2.5782	2.2956
PSNR(dB)	9.2500	16.3790	21.9705	24.2088	26.3013	29.0224	31.1971	32.6288	33.2844	33.5130
MSE	7.7282e+003	1.4969e+003	413.0728	246.7156	152.3879	81.4396	49.3591	35.4974	30.5239	28.9588
bpp	0.5386	1.2982	1.5000	1.5219	1.6049	1.8367	2.2723	2.9937	4.2098	4.8447
CR %	93.2678	83.7719	81.2500	80.9761	79.9385	77.0412	71.5958	62.5786	47.3774	39.4409

The decoded images at the end of passes 6, 7 and 8 are shown in figure 5.11.

(a) Thr=27, PSNR=29.0224 (b) Thr=14, PSNR=31.1971 (c) Thr=7, PSNR=32.6288

Figure 5.11(a)-(c) Decoded Images of passes 6 to 8 of Coding Scheme C, DRP=3

(ii) Detail Retaining Pass Number (DRP) = 4

The total execution time in sec. of 10 Dominant passes, without estimating subordinate pass time, is 50.9291 sec. The results of various parameters over 10 passes are shown in table-X.

Table-X: Parameter of Coding Scheme C with DRP=4 on Pirate Image

Test Img. Pirate/thr.	1 Thr=871	2 Thr=436	3 Thr=218	4 Thr=109	5 Thr=54	6 Thr=27	7 Thr=14	8 Thr=7	9 Thr=3	10 Thr=2
Execution Time(sec.)	15.6270	3.9230	4.4351	4.4721	5.1763	5.6656	3.6131	3.1032	2.5775	2.2909
PSNR(dB)	9.2500	16.3790	21.9705	24.2088	26.3085	29.0685	31.2839	32.7495	34.7254	33.6619
MSE	7.7282e+003	1.4969e+003	413.0728	246.7156	152.1344	80.5801	48.3831	34.5251	29.5489	27.9828
bpp	0.5386	1.2982	1.5000	1.5068`	1.5906	1.8239	2.2613	2.9840	4.2009	4.8359
CR %	93.2678	83.7719	81.2500	81.1646	80.1170	77.2007	71.7339	62.6995	47.4888	39.5512

The decoded images at the end of passes 6, 7 and 8 are shown in figure 5.12.

(a) Thr=27, PSNR=29.0685 (b) Thr=14, PSNR=31.2839 (c) Thr=7, PSNR=32.7495

Figure 5.12(a)-(c) Decoded Images of passes 6 to 8 of Coding Scheme C, DRP=4

(iii) Detail Retaining Pass Number (DRP) = 5

The total execution time in sec. of 10 Dominant passes, without estimating subordinate pass time, is 52.1317 sec. The results of various parameters over 10 passes are shown in table-XI.

Table-XI: Parameter of Coding Scheme C with DRP=5 on Pirate Image

Test Img. Pirate/thr.	1 Thr=871	2 Thr=436	3 Thr=218	4 Thr=109	5 Thr=54	6 Thr=27	7 Thr=14	8 Thr=7	9 Thr=3	10 Thr=2
Execution Time(sec.)	15.6270	3.9230	4.4351	4.4721	5.1763	5.6656	3.6131	3.1032	2.5775	2.2909
PSNR(dB)	9.2500	16.3790	21.9705	24.2088	26.3402	29.2391	31.6640	33.3258	34.1160	34.3963
MSE	7.7282e+003	1.4969e+003	413.0728	246.7156	151.0291	77.4757	44.3287	30.2340	25.2047	23.6290

bpp	0.5386	1.2982	1.5000	1.5068`	1.5566	1.7967	2.2474	2.9819	4.2098	4.8476
CR %	93.2678	83.7719	81.2500	81.1646	80.5424	77.5410	71.9070	62.7262	47.3770	39.4054

The decoded images at the end of passes 6, 7 and 8 are shown in figure 5.13.

(a) Thr=27, PSNR=29.2391 (b) Thr=14, PSNR=31.6640 (c) Thr=7, PSNR=33.3258

Figure 5.13(a)-(c) Decoded Images of passes 6 to 8 of Coding Scheme C, DRP=5

5.3.2(d) Discussion

For the purpose of analysis the execution time of dominant pass up to different number of passes has been recorded and shown in table-XII. The effect of changing the algorithm to improve execution time is analyzed with respect to the image quality obtain thereby.

Table-XII: Execution Time of Dominant Passes recorded uptill different iterative passes in sec.

Scheme →	A	B	C, DRP=3	C, DRP=4	C, DRP=5
Pass 6	31.5749	41.0908	40.0971	39.4836	41.0091
Pass 7	33.8431	45.2289	43.8391	42.0070	44.7187
Pass 8	35.9524	48.6338	46.8354	45.1400	48.4207
Pass 9	37.8126	52.4482	49.2567	49.9085	49.8757
Pass 10	39.4757	55.0811	51.4581	51.3345	52.1317

The PSNR of Pirate image obtained after decoding at subordinate pass of different algorithms has been plotted in figure 5.14, for different iterative passes.

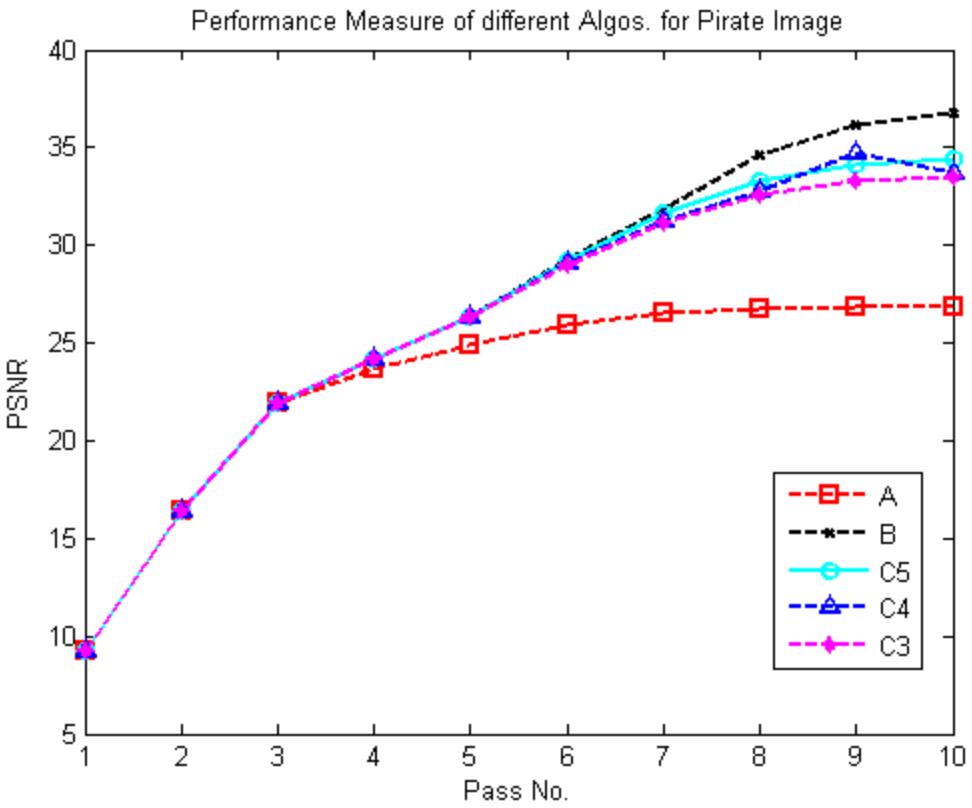

Figure 5.14 PSNR plot of uncompressed decoded Pirate Image at different iterative

It can be can be clearly seen from table-XII that in all 6 iterative passes the proposed algorithm C saves around a second for all variations in DRP as compared to idle coding scheme B. Also it can be seen from table-VIII, IX, X and figure 5.14 that PSNR values at the output of 6th iterative pass are almost same. It can be inferred from table-XII that there is an improvement of 2 sec. in the execution of total 7 iterative passes of proposed coding C when compared with idle coding scheme B. It can be seen that at the end of 8 iterative passes the improvement in time is around 3 seconds. The difference of 3 sec. or more is maintained there after 8 iterative passes.

From plot of PSNR in figure 5.14 it can be seen that there is a little fall in PSNR at 7th iterative pass in coding scheme C as compared to coding scheme B. It can be seen from table-VIII, IX, X and XI that this variation is less than 1 dB and is around 0.2-0.6 dB. At the 8th iterative pass the difference of 2dB comes up in coding algorithm C with DRP=3 as compared with coding scheme B. At DRP=5 the difference is 1 dB, which can be seen from table-VIII and XI, but the time improvement is less.

At 8^{th} , 9^{th} and 10^{th} iterative passes the threshold becomes very less. It is 7, 3 and 2 respectively. The threshold of 7 explains that why there is a fall in PSNR values at the 8^{th} iterative pass. The threshold is much nearer to 0 as compared with initial threshold of 871. For 9^{th} and 10^{th} iterative passes it becomes even lower. Thus, the assumption that the descendants of zero-tree roots have nearly zero magnitude coefficients becomes null. Still at higher passes there are many coefficients near to zero as can be seen from the compression ratio of 47.47% and 36.09% for passes 9 and 10 in table-VIII, but the coefficients becoming significant at such small thresholds of 3 and 2 add to significant details which improves the PSNR to a greater extent.

Thus for the given test image the proposed coding scheme C works well up till 7 iterative passes; and give the improvement of 2 sec. in execution time up to 7 iterative passes. In execution of collective 8 iterative passes the improvement of 3 sec. in execution time comes up but the fall in PSNR is a little higher in the Pirate image as compared to the Elaine image. At passes 9 and above coding scheme B is preferred due to higher PSNR values at low thresholds.

5.3.3 Results on test image3 – Jet

The Jet image of Size 512 x 512 was taken as the second test image.

Figure 5.15 Test Image3-'Jet'

5.3.3(a) Coding Scheme A

The Coding Scheme A was applied over the Jet image for 10 passes and various parameters were recorded including the execution time of the dominant pass.

The total execution time in sec. of 10 Dominant passes, without estimating subordinate pass time, is 64.8164 sec. The results of various parameters over 10 passes are shown in table-XIII.

Table-XIII: Parameter of Coding Scheme A on Jet Image

Test Img. Jet/thr.	1 Thr=840	2 Thr=402	3 Thr=201	4 Thr=101	5 Thr=50	6 Thr=25	7 Thr=13	8 Thr=6	9 Thr=3	10 Thr=2
Execution Time(sec.)	26.0031	4.5000	4.4726	4.4776	4.7110	4.5870	4.4941	4.5274	3.9517	3.0527
PSNR(dB)	4.8170	10.3405	22.8622	26.8480	29.8228	31.8740	32.6167	33.0366	33.3224	33.5134
MSE	2.1448e+004	6.0121e+003	336.4045	134.3633	67.7323	42.2362	35.5966	32.3164	30.2583	28.9559
bpp	1.4735	1.4753	1.4769	1.4819	1.5018	1.5569	1.6586	1.9416	2.7367	3.5611
CR %	81.5815	81.5590	81.5384	81.4758	81.2275	80.5382	79.2675	75.7298	65.7917	55.4859

The decoded images at the end of passes 6 to 8 are shown in figure 5.16

(a) Thr=25, PSNR=31.8740 (b) Thr=13, PSNR=32.6167 (c) Thr=6, PSNR=33.0366

Figure 5.16(a)-(c) Decoded Images of passes 6 to 8 of Coding Scheme A

5.3.3(b) Coding Scheme B

The Coding Scheme B was applied over the Jet image for 10 passes and various parameters were recorded including the execution time of the dominant pass.

The total execution time in sec. of 10 Dominant passes, without estimating subordinate pass time, is 70.3173 sec. The results of various parameters over 10 passes are shown in table-XIV.

Table-XIV: Parameter of Coding Scheme B on Jet Image

Test Img. Jet/thr.	1 Thr=840	2 Thr=402	3 Thr=201	4 Thr=101	5 Thr=50	6 Thr=25	7 Thr=13	8 Thr=6	9 Thr=3	10 Thr=2
Execution Time(sec.)	25.8775	4.4186	4.4409	4.4695	9.0107	4.8723	4.3823	4.4743	4.4548	3.7946
PSNR(dB)	4.8170	10.3405	22.8689	27.0267	30.4466	33.3999	34.7662	35.8708	36.8003	37.4405
MSE	2.1448e+004	6.0121e+003	335.8849	128.9476	58.6704	29.7226	20.7232	16.3305	13.5848	11.7227
bpp	1.4735	1.4933	1.5013	1.5053	1.5234	1.5769	1.6846	1.9991	2.9355	3.8951
CR %	81.5815	81.3339	81.2332	81.1832	80.9570	80.2883	78.9429	75.0111	63.3064	51.3107

The decoded images at the end of passes 6 to 8 are shown in figure 5.17

(a) Thr=25, PSNR=33.3999 (b) Thr=13, PSNR=34.7662 (c) Thr=6, PSNR=35.8708

Figure 5.17(a)-(c) Decoded Images of passes 6 to 8 of Coding Scheme B

5.3.3(c) Proposed Coding Scheme C

The Coding Scheme C was applied over the Jet image for 10 passes and various parameters were recorded included the execution time by setting Detail Retaining Pass Number different each time.

(i) Detail Retaining Pass Number (DRP) = 3

The total execution time in sec. of 10 Dominant passes, without estimating subordinate pass time, is 64.1190 sec. The results of various parameters over 10 passes are shown in table-XV.

Table-XV: Parameter of Coding Scheme C with DRP=3 on Jet Image

Test Img. Jet/thr.	1 Thr=840	2 Thr=402	3 Thr=201	4 Thr=101	5 Thr=50	6 Thr=25	7 Thr=13	8 Thr=6	9 Thr=3	10 Thr=2
Execution Time(sec.)	25.9802	4.3987	4.4224	4.3927	4.7002	4.5769	4.3612	4.4364	3.8306	2.9775
PSNR(dB)	4.8170	10.3405	22.8689	27.0267	30.3685	33.0175	34.1709	34.8477	35.3121	35.6251
MSE	2.1448e+004	6.0121e+003	335.8849	128.9476	59.7357	32.4585	24.8880	21.2966	19.1367	17.8062
bpp	1.4735	1.4933	1.5013	1.5074	1.5314	1.5962	1.7108	2.0120	2.8243	3.6574
CR %	81.5815	81.3339	81.2332	81.1569	80.8575	80.0480	78.6156	74.8505	64.6957	54.2820

The decoded images at the end of passes 6, 7 and 8 are shown in figure 5.18.

(a) Thr=25, PSNR=33.0175 (b) Thr=13, PSNR=34.1709 (c) Thr=6, PSNR=34.8477

Figure 5.18(a)-(c) Decoded Images of passes 6 to 8 of Coding Scheme C with DRP=3

(ii) Detail Retaining Pass Number (DRP) = 4

The total execution time in sec. of 10 Dominant passes, without estimating subordinate pass time, is 63.9203 sec. The results of various parameters over 10 passes are shown in table-XVI.

Table-XVI: Parameter of Coding Scheme C with DRP=4 on Jet Image

Test Img. Jet/thr.	1 Thr=840	2 Thr=402	3 Thr=201	4 Thr=101	5 Thr=50	6 Thr=25	7 Thr=13	8 Thr=6	9 Thr=3	10 Thr=2
Execution Time(sec.)	15.6270	3.9230	4.4351	4.4721	5.1763	5.6656	3.6131	3.1032	2.5775	2.2909
PSNR(dB)	4.8170	10.3405	22.8689	27.0267	30.3924	33.1010	34.2894	34.9873	35.4677	35.7925
MSE	2.1448e+004	6.0121e+003	335.8849	128.9476	59.4077	31.8404	24.2182	20.6230	18.4633	17.1327

bpp	1.4735	1.4933	1.5013	1.5053	1.5302	1.5960	1.7113	2.0132	2.8258	3.6591
CR %	81.5815	81.3339	81.2332	81.1832	80.8731	80.0503	78.6083	74.8352	64.6778	54.2618

The decoded images at the end of passes 6, 7 and 8 are shown in figure 5.19.

(a) Thr=25, PSNR=33.1010 (b) Thr=13, PSNR=34.2894 (c) Thr=6, PSNR=34.9873

Figure 5.19(a)-(c) Decoded Images of passes 6 to 8 of Coding Scheme C with DRP=4

ii) Detail Retaining Pass Number (DRP) = 5

The total execution time in sec. of 10 Dominant passes, without estimating subordinate pass time, is 68.3722 sec. The results of various parameters over 10 passes are shown in table-XVII.

Table-XVII: Parameter of Coding Scheme C with DRP=5 on Jet Image

Test Img. Jet/thr.	1 Thr=840	2 Thr=402	3 Thr=201	4 Thr=101	5 Thr=50	6 Thr=25	7 Thr=13	8 Thr=6	9 Thr=3	10 Thr=2
Execution Time(sec.)	26.0153	4.3978	4.4020	4.4606	9.0361	4.3463	4.3669	4.4635	3.8595	2.9812
PSNR(dB)	4.8170	10.3405	22.8689	27.0267	30.4466	33.3228	34.6502	35.4371	35.9804	36.3491
MSE	2.1448e+004	6.0121e+003	335.8849	128.9476	58.6704	30.2553	22.2877	18.5938	16.4074	15.0721
bpp	1.4735	1.4933	1.5013	1.5053	1.5234	1.5932	1.7130	2.0208	2.8375	3.6724
CR %	81.5815	81.3339	81.2332	81.1832	80.9570	80.0854	78.5873	74.7398	64.5309	54.0951

The decoded images at the end of passes 6, 7 and 8 are shown in figure 5.20.

(a) Thr=25, PSNR=33.3228 (b) Thr=13, PSNR=34.6502 (c) Thr=6, PSNR=35.4371

Figure 5.20(a)-(c) Decoded Images of passes 6 to 8 of Coding Scheme C with DRP=5

5.3.3(d) Discussion

For the purpose of analysis the execution time of dominant pass up to different number of passes has been recorded and shown in table-XVIII. The effect of changing the algorithm to improve execution time is analyzed with respect to the image quality obtain thereby.

Table-XVIII: Execution Time of Dominant Passes recorded uptill different iterative passes in

Scheme →	A	B	C, DRP=3	C, DRP=4	C, DRP=5
Pass 6	48.9855	53.1521	48.5977	48.4548	53.4361
Pass 7	53.3927	57.3746	52.6741	53.0773	56.9992
Pass 8	57.8879	61.9831	57.3048	57.1115	61.3733
Pass 9	61.5699	66.4705	61.2281	61.4803	65.1374
Pass 10	64.8164	70.3173	64.1190	63.9203	68.3722

The PSNR of Pirate image obtained after decoding at subordinate pass of different algorithms has been plotted in figure 5.21, for different iterative passes.

It can be clearly seen from table-XVIII that the execution time for the dominant pass has been greatly improved by proposed algorithm C for Detail Retaining Pass (DRP) 3 and 4. Though for DRP = 5 time taken is almost same as that taken by coding scheme B. At times coding scheme A is not taken into comparison because the PSNR values obtained by A are low; but it is the base of proposed coding algorithm C. From table-XVIII it can be seen that for 6, 7 and 8 successive

iterative passes coding scheme C saves 4 sec. or little more for DRP= 3 and 4 when compared with coding scheme B. But the execution time taken is almost the same as B when DRP = 5.

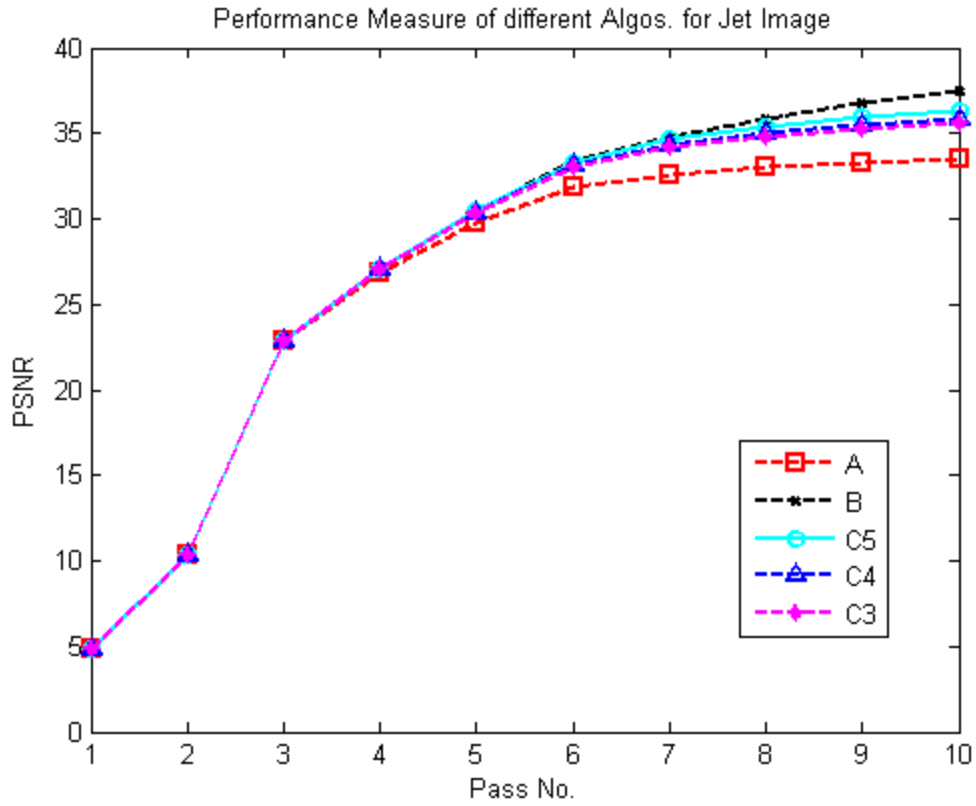

Figure 5.21 PSNR plot of uncompressed decoded Jet Image at different iterative passes

It can be clearly seen from figure 5.20 that uptill 6th iterative pass the PSNR of the decoded uncompressed images are almost same for coding scheme C and B. This can also be verified from table-XIV, XV, XVI and XVII. From the same tables and the figure plot 5.21 it can be seen that at 7th iterative pass PSNR falls a little. This fall is always less than 0.6 dB for all cases of coding scheme C when compared with B. From table-XIV, XV, XVI, XVII and figure 5.21 it can bee seen that in the 8th iterative pass the fall in PSNR of decoded images of scheme C is around 1 dB as compared with that of B, but the execution time is improved by 1 more second.

Thus for the given test image coding scheme C works best for 7 iterative passes and saves 4 seconds in the execution of dominant pass. If a fall of 1 dB is allowed 8 successive iterative passes can save 1 more second. For passes 9 and above the zero magnitude assumption of the descendants is nullified since the thresholds become very small and coding scheme B gives better results there on.

Chapter 6

Conclusion

The thesis presents a new way to improve the encoding time of Embedded Zero-tree Wavelet (EZW) Coding by reducing the execution time of the dominant pass in the algorithm. It has been shown in the thesis that the assumption of zero-tree roots having descendants of nearly zero magnitude works well after the third dominant pass. It is concluded from the results that the proposed algorithm C saves 2 seconds or more in successive execution of 7 dominant passes, without calling subordinate passes. Also the compression ratio is improved by 2% in most of the images. Since no changes in the subordinate pass have been made, the contribution of subordinate passes remains the same. The PSNR of the decoded image of proposed coding almost remains the same as obtained from EZW coding.

It can been concluded from the results that an improvement of 1 second more can be made by the proposed coding in the 8 successive dominant passes if a fall of 1 dB, compared to EZW coding is allowed. The decoded image can be brought into 1 dB range, if not, by choosing a proper Detail Retaining Pass (DRP). The proposed descendant magnitude approximation is applied after the chosen DRP. The proper selection of DRP can be made by evaluating the threshold of the 8^{th} dominant pass. If the threshold is nearer to10 in the 8^{th} pass, like 8 or 9 the DRP should be made 3 but if the threshold is more nearer to 5, like 6 or 7 the DRP should be shifted to 4.

For passes higher than 8, the threshold becomes very small as compared with initial thresholds. It is around 3 or less. Thus the approximation that the descendants of zero-tree roots have nearly

zero magnitude and will not become significant in successive passes is nullified. Hence, the proposed coding scheme C is constrained to 8^{th} dominant pass.

On the simulated software and hardware the proposed coding scheme gives an execution time reduction of about 3 seconds up to 8 successive passes, with constraints. This could be different on other simulating systems. It should be stated that if the proposed coding scheme gives the same decoded output in terms of PSNR and other performance indexes as compared with conventional EZW, the proposed coding scheme will always take less time to execute because the coefficient-trees of large number of descendants of zero-tree roots of the previous passes have not been scanned for the determination of zero-tree roots and isolated zeros.

The future scope of the proposed work lies in the improvement of video codecs such as MPEG-4 based on EZW and other wavelet transforms based video codecs. Frame rates are very important in video compressions. Reduced execution time of EZW will directly have an effect on video codecs and video streaming. Higher rates are possible on the same bit-per-pixel.

The proposed coding will improve the functioning of small processors; such as those in mobiles which work on multimedia processing and applications.

References

[1] K.P. Soman; K.I. Ramchandran; "Insight into Wavelets – From Theory to Practice", *Prentice Hall of India*, Second Edition, pp. 6-9, 2005

[2] S. Mallat; "A theory for multiresolution signal decomposition: The wavelet representation," *IEEE Trans. Patr. Anal. Machine Intell.*, vol. 11, no. 7, pp. 674-693, July 1989

[3] I. Daubechies; Ten Lectures on Wavelets, *SIAM*, 1992

[4] K.P. Soman; K.I. Ramchandran; "Insight into Wavelets – From Theory to Practice", *Prentice Hall of India*, Second Edition, pp. 83, 2005

[5] M. Antonini, *et.al.:* "Image Coding Using Wavelet Transforms" *IEEE Trans. Image Processing*, vol. 1, no. 2, pp 205-220, April 1992

[6] J.M. Shapiro; "Embedded Image Coding Using Zerotrees of Wavelet Coefficients" *IEEE Trans. on Signal Processing*, vol. 41, issue 12, pp 3445-3462, 1993

[7] A. Manduca; "Compressing Images with Wavelet/Subband Coding", *Engineering in Medicine and Biology Magazine, IEEE*; vol. 14, no. 5, pp. 639-646, 1995

[8] Amir Averbuch, *et.al.:* "Image Compression Using Wavelet Transform and Multiresolution Decomposition", *IEEE Trans. Image Processing*; vol. 5, no. 1, pp 4-15, January 1996

[9] A. Munteanu; *et.al*: "Wavelet-Based Lossless Compression of Coronary Angiographic Images", *IEEE Trans. Medical Imaging*; vol. 18, no.3, pp. 272-281, 1999

[10] L. Kaur; *et.al*: "Compression of Medical Ultrasound images using Wavelet Transform and Vector Quantization", *IEEE EMBS Asian-Pacific Conf. on Biomedical Engineering, 2003*; pp. 170-171, 2003

[11] T. Guowei, *et.al:* "An Improved EZW Image Coding Method Based on Lifting Wavelet"; *Int. Conf. on Wireless Communications, Networking and Mobile Computing*, pp. 2897-2899, 2007

[12] L. Xuhong; *et.al:* "Improved Image Coding Algorithm Based on Embedded Zerotree"; *Eighth ACIS Int. Conf. on Software Engineering, Artificial Intelligence, Networking, and Parallel/Distributed Computing* , vol. 2, pp. 189-192, 2007

[13] P. Bharti; *et.al:* "Comparative Analysis of Image Compression Techniques: A Case Study on Medical Images", *Int. Conf. ARTcom'09, IEEE Conf.*; pp. 820-822, 2009